Small Scale Folding in NEEM Ice Core

Bachelor Thesis

Submitted: August $20^{\text{th}}, 2014$

at
**Eberhard Karls Universität
Tübingen**
and
**Alfred Wegener Institute
Helmholtz Center for Polar and Marine Research
Bremerhaven**

Name: Julien Westhoff
1st Supervisor: Prof Dr Ilka Weikusat
2nd Supervisor: Prof Dr Paul Bons

Declaration of Authorship

I, Julien Westhoff, hereby declare that I have written this bachelor thesis on my own and without others than the indicated sources. All passages and phrases which are literally or in general taken from publications, books or other sources are marked as such.

Tübingen, August 20$^{\text{th}}$, 2014

_____

Julien Westhoff

Abstract

NEEM is a drilling site in north western Greenland, from which a 2500 m long ice core has been derived. The ice has been analyzed with visual stratigraphy to make layering visible. This thesis analyzes the layering from top to bottom in terms of folding events. Small disturbances of layers start to appear around 1560 m depth and folding is visible at 1750 m depth from the surface. Below 2160 m there has been so much deformation that a qualitive description is not possible. From 1750 m to 2160 m there is an evolution of folding, where normal folds, then Z-folds and shear zones, and in greater depths many Z-folds in one layer appear. They are a result of increasing strain rate, leading to deformation, which in this depth is mainly ductile. Fold types with a brittle component are also visible in form of detachment folds. The dominant structures are Z-folds located at shear zones which were created by deformation, resulting in these diagonal shear zone in the core. These shear zones have also been analyzed with the fabric analyzer to find the main c-axis orientation within these zones. The main orientation is caused by a tilting of the grains during deformation and another part due to recrystalization processes. The orientation of these shear zones can be estimated by using the linescanner images which show the ice in different focus depths in the horizontal level of the core and reveal a general orientation to the top left of the images, caused by shear stress from the right in a small angle.

Zusammenfassung

NEEM ist ein Standort und der Name des 2500 m langen Eisbohrkerns aus Grönland. Dieser Kern wurde mit dem Linescanner analysiert und es entstanden Bilder des gesamten Kerns, welche die Schichtung des Eises zeigen und mit der Methode der *Visual Stratigraphy* sichtbar gemacht wurden. Die sehr parallele Schichtung wird ab etwa 1560 m Tiefe von kleinen Wellen gestört und ab 1750 m befinden sich eindeutige Falten im Bohrkern. Durch die steigende Deformationsrate ist eine qualitative Auswertung der Faltenstrukturen unterhalb 2160 m nicht möglich. In einer Tiefe von 1750 m bis 2160 m entwickeln sich normalen Falten, hin zu Z-Falten, bis hin zu Schichten mit mehreren Z-Falten und Scherzonen. Dies geschieht durch die steigende Deformationsrate, welche zu duktiler Deformation führt. Spröde Deformation ist in *detachment folds* (wörtlich: Trennungs-Falten) zu sehen; die dominanteste Struktur sind aber Z-Falten, welche auf einer Scherzone liegen. Diese Scherzonen wurden mit dem *Fabric Analyzer* abgebildet und zur Bestimmung der c-Achsenorientierung ausgewertet. Die generelle Orientierung in diesen Zonen entsteht durch eine Verkippung während der Deformation; einige Körner sind jedoch das Ergebnis späterer Rekristallisation. Die Orientierung der gesamten Scherzone wurde mit Linescannerbildern erzeugt, welche den Kern in der Horizontalen in verschiedenen Tiefen fokussiert hatten. Dies zeigt eine generelle obenlinks-untenrechts Orientierung der Scherzone in den Bilder, welche durch eine Kraft von rechts entstanden sind.

Acknowledgments

Contents

List of Figures

Chapter 1

Introduction

1.1 Motivation

Ice is very common and used in everyday life, yet it is a major subject of research where new knowledge is constantly gained. During the work on my bachelor thesis at the Alfred-Wegener-Institut (AWI) in Bremerhaven, I had the opportunity to contribute to current research, especially in the field of physical properties of ice.

In geological terms, ice is considered to be a rock, rather than a fluid, which therefore combines the fields of Geology and Glaciology. In Geology folds have been observed and described for many years, but in Glaciology they have not yet played a very big role. To compute to recent studies, I will take on the questions: "At which depth of the ice sheet does folding occur?", "Is folding visible and –if so– at what scale?" and "Is it possible to quantify and characterize these small scale folds?".

These questions came up recently as a large scale fold was discovered in the bottom part of the NEEM (Northern Greenland Eemian Ice Drilling) ice core and small scale folds have not been qualitatively examined. Considering this, this is a good topic for a bachelor thesis.

1.2 Properties of Ice

Compared to other rocks, ice is a material that is very close to its melting point at natural conditions on the surface of the earth. Its solidus lays around $0\,^{\circ}$C. It has a much lower density then, e.g. Quarz (ca. 2650 kg/m^3), with ca. 917 kg/m^3 in the solid state without air bubbles (*Kuhs, 2007*).

Ice is a material made of the elements hydrogen and oxygen and has its

solid state below 0 °C. Its crystal system is hexagonal, with the basal planes perpendicular to the c-axis. With increasing depth in an ice sheet the grains start to reorientate and align their c-axes vertically. This creates basal planes parallel to the ice's surface, which are the main source of deformation, known as basal sliding (*Surma, 2011; Eichler, 2013*).

Another crystallographic property is the high anisotropy. This means that the properties of ice are highly dependent on its crystallographic direction. This is important for the deformation processes, where sliding mainly occurs parallel to the basal planes (*Thorsteinsson, 2000*).

Motion of ice is also visible on a large scale, where ice sheets strech out to the ocean and there break off, which is known as calving. Parts of the ice moving down the slope are known as glaciers. They start with accumulation of snow and ice and then move away from the ice divides or domes down the slopes, mostley towards the ocean. During their descent it comes to a lot of internal deformation of the ice (*Benn, 2010*).

1.3   NEEM Ice Core

Figure 1.1: *Map of Greenland showing the location of NEEM (from NEEM homepage).*

NEEM is the name of a drilling site in Greenland (location: 77.45 ° N, 51.06 ° W), where a 2540 m long core of ice was drilled in the years from 2008 to 2012 (*NEEM community, 2013*). The aim of this drilling was to find ice from the last interglacial period, the Eemian (-EEM), on the northern hemisphere (N-). The corresponding ice from the southern hemisphere was, e.g. derived from Vostok or Dome C (*Surma, 2011*) drillings in Antarctica. Every 55 cm have been put into a new bag and numbered continuously from top to bottom.

The location for NEEM was chosen on an ice devide orientated NW-SE, where the biggest gradients are SW and NE. Here the ice has a thickness of 2542 m and the Eemian is expected to be found in a depth of 2265 m to 2345 m (*NEEM community, 2013*). Below 2207 m (108 ka) the layering is strongly disturbed, this is where the Eemian (115 - 130 ka) should be found. One of the main goals of the drilling

was to find an undisturbed ice record, but as the NEEM comunity members describe in *Nature* (*NEEM comunity, 2013*), we see folding in this part of the core too and thus a doubling in the chronological layering. With these results folding in ice became a relevant topic. As this thesis will analyse and discuss the evolution of the folding from top to bottom in this core, I will later refer to the Eemian ice again. First the following chapter will give an introduction to geological folding, focused on the relavant fold types for ice.

1.4 Folds in Geology

1 How Folding Occurs

Folding is a geolgoical structure which is created by bending of units, which is easiest to be seen in layered material. Probably the first person to describe folds in rocks was Hall (*Hall, 1815*), wo compared these with models he made from cloth between boards (*Schmalholz, 2001*). Folding can occur on all scales, from submicroscopic to tens of kilometers and is mostly the result of a compressive stress regime. Yet in some cases folding is the result of elongation (*Davis, 2011*).

2 Types of Folds
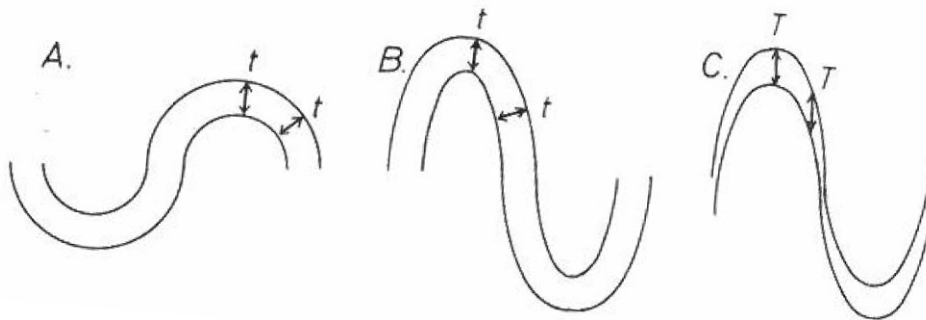
Figure 1.2: *Geometric features of: A, concentric parallel folds; B, non-concentric parallel folds; and C, similar folds. Orthogonal layer thickness t; layer thickness parallel to axial plane T (from Ramsay, 1987).*

3

In general folds can be divided into two groups, parallel folds and similar folds (*Van Hise, 1896*). In parallel folds the thickness t is measured orthogonally between the layer boundaries and is constant throughout the fold (Fig. 1.2 B). Parallel folds are generally found in layers with high competence contrasts. Similar folds, in contrast to parallel folds, show considerable variations of layer thickness and always a thinning of the fold limbs relative to that seen at the hinge zone, as to be seen in fig. 1.2 C (*Ramsay, 1987*).

Competence is the resistance of a rock against deformation, and competence contrast defines the differences in hardness of two materials. High competence contrasts from 1:20 result in folds like Fig. 1.2 A and B, small differences, e.g. 1:3 result in folds as shown in Fig. 1.2 C.

In summary, parallel folds, also known as buckle folds, occur in zones with layers of high competence contrast, where on the other hand, simple or passive folds are the result of simple shear. The method of distinguishing these will be explained in the next section.
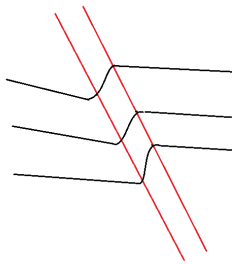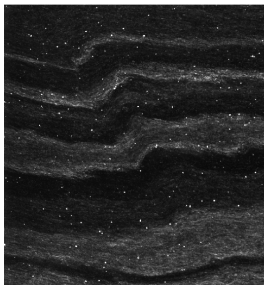
Figure 1.3: *Left is a excerpt from bag 3208 at bag depth 55 cm (1764 m below surface); right is the sketch of the layer boundaries (black) and the fold axis (red) with the shear zone between the two red lines (not marked in color).*

For further understanding it is necessary to define expressions used later. *Well-layered* or *well-stratigrified* means that the layer boundaries are all parallel. *Small waves* are the first disturbances in the well layered ice and represent a wavy or slightly curved character of the boundaries. A fold, referred to as *normal fold* is a 'wave' in the layers as it is seen in Fig. 1.2.

Z-folds have their name from the 'Z' form of the fold. Fig. 1.3 idealized Z-fold in black. With the fold axis in red, which is the angle biscector of the fold, and the *shear zone* located between the two red lines, which is the area of deformation in a ductile surrounding.

3 Measuring and Plotting Layer Thickness Variations
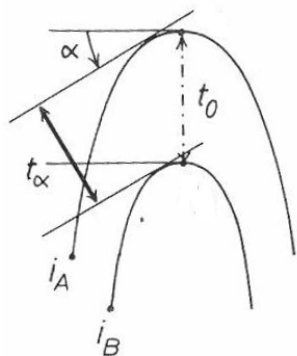
Figure 1.4: *Method to determine the orthogonal layer thickness t_α at angle of dip α. i_A and i_B represent a sketched layer's boundary and t_0 is maximal distance in the hinge zone (modified from Ramsay, 1987).*

Ramsay gives a detailed description of how to determine the layer thickness and calculate the angle of dip (*Ramsay, 1967*). This detailed description would lead too far, where the important result is basically the ratio between t_α and T_α (Fig. 1.4). With this we can calculate the vaule $t'_\alpha = cos\alpha$.

This can be plotted in a graph with α against the orthogonal thickness t'_α. This leads to three classes of folds and my aim is to characterize the folding in ice with this graph.

The sketches on the right side of fig. 1.5 show characteristic folds with a decrease in competence contrast from top to bottom. To fig. 1.5 will be referred again in chapter 2.4 as a part of the interpretation of the folding throughout the core.
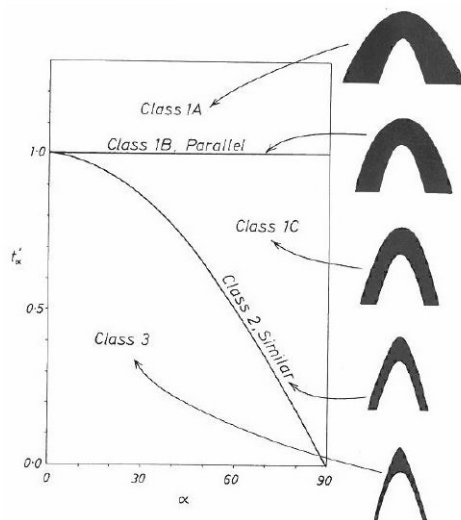
Figure 1.5: *Standardized orthogonal thickness t_α plotted against the angle of dip α and the main type of fold classes (modified from Ramsay, 1987).*

1.5 Previous Work on Micro and Macro Scale Folds in Ice
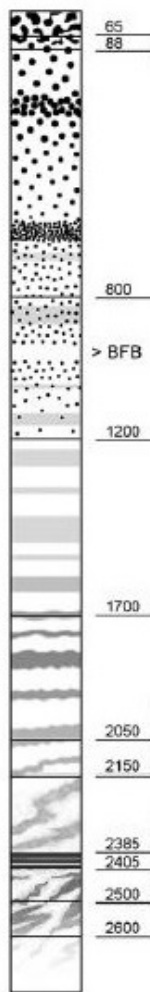
Figure 1.6: *Shematic outline of VS images throughout EDML ice core from Antarctica. Numbers on right represent the depth in meters (modified from Faria, 2010).*

In early drillings in ice small scale folding has been observed. Yet for the reconstruction of the climate record it did not appear to be of relevance and has therefore been ignored. Many authors describing the layering in the cores from Greenland and Antarctica have just mentioned these small folds with a few sentences: "Below this depth smaller disturbances in the layering such as micro folds start to appear (...). Such disturbances were also observed in the deep parts of the GISP2 and GRIP ice cores" (*Svensson, 2004*). No serious attempt has been made to classify these even though they are mentioned in previous publications.

Sérgio Faria shows how the Visual Stratigraphy (VS) looks in every depth of the core and Z-folds are the dominant feature in a depth from 2150 m (*Faria, 2010*). These are visualized in fig. 1.6.

1.6 Large Scale Fold in NEEM

Research by the NEEM community has shown that there must be a large scale fold (*NEEM community, 2013*) in the bottom part of the core (below 2200 m). This was discovered by a doubling of the isotope signals in these parts of the core. By overlapping these signals, plotted in a graph, the authors verified their statement. Yet this is the only evidence for a large scale fold in this strongly sheared and deformed bottom part of the core. Additionally it is hard to follow such a fold over a large scale, because there is just one locally restricted borehole and radar methods have not yet revealed this large overturned fold. The radar methods have revealed some layering in the bottom meters of the core and on the x-axis strongly shortened images are used to show general folding.

The chapter "2.2 Results: Where Folding Occurs" will show that folding occurs at a depth above 2200 m. For this I will analyze the small scale folding using the linescanner images. First, the chapter "2.1 Method: Visual Stratigraphy" will give a short intoduction to the method of visulising layers in the ice core.

Chapter 2

Folds in Ice

2.1 Method: Visual Stratigraphy
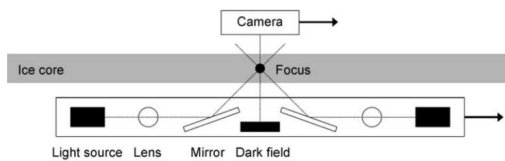
Figure 2.1: *Array of the camera to detect the refraction of light as the camera is moved along the length of the core (from Svensson, 2004).*

As ice is mostly clear it is necessary for stratigraphy to make a layering visible. This is done with the line scanner camera using the method of visual stratigraphy (VS), where a camera array is chosen to make the impurities visible (Fig. 2.1). With this array, ice, that is very clear, will appear black, as no light is refracted on particles. Ice which contains impurities will appear increasingly bright and will visualize cloudy bands (i.e. 'brighter' layers in the image). The occurence of cloudy bands in glacial ice with high concentrations of dust and other impurities has long been recognized (e.g. *Ram and Koenig, 1997*) and today it is possible to create high resolution pictures of these, taking advantage of the large storage capability of modern computers. Due to that VS is recently applied to all cores.

Svensson shows how VS is applied on NorthGRIP and describes the method in detail (*Svensson, 2004*). The visualizations he produces are very similar to the ones found in the VS data of NEEM, which therefore justifies this comparison. The NEEM linescan pictures were produced in the ice lab of the AWI in Bremerhaven, Germany, stored on the webpage *www.pangaea.de* and published by Sepp Kipfstuhl (*Kipfstuhl, 2010*).

2.2 Results: Where Folding Occurs
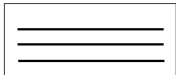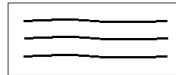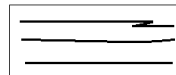
Depth Region	Bag	Depth	Description	Schematic image
1	0	0	no folding	
	2838 —	1560		
2			small waves	
	3189 —	1750		
	3274	1800		
	3364	1850		
	3456	1900	folding	
3	3546	1950		
	3636	2000		
	3728	2050		
	3818	2100		
	3930 —	2160		
4			sheared	
	4600 —	2530		

Figure 2.2: *Gives an overview of 'depth regions', 'bag numbers', 'depth', 'folding' and a sketch of the image at that depth.*

As Faria (*Faria, 2010*) shows in his graph for an Antarctic core (Fig. 1.5), folding occurs from 2050 m to 2385 m. The depth is similar in Greenlands NEEM core. Here we have the beginning of folding in a depth of 1750 m (Overview shown in fig. 2.2), where we can see the occurence of waves in the cloudy bands. These later evolve to normal folds, then asymmetrical Z-folds which also create shear zones below them. Z-folds, i.e. overturned normal folds, become the most dominant type of folding in the deeper parts of the core. At a depth of 2160 m, Z-folding is so far advanced that the fold axis cannot be seen anymore in the width of the core.

As folding has been observed and confirmend in depths deeper than 2200 m, I will now give a detailed description of the folding in the layers above 2200 m. Beginning above 1560 m, where we see no folding, through the depth of 1750 m, where folding begins, until 2160 m, where folding is so disturbed, that it is no longer possible to give a cm-exact description of the folds.

1 Depth Region 1
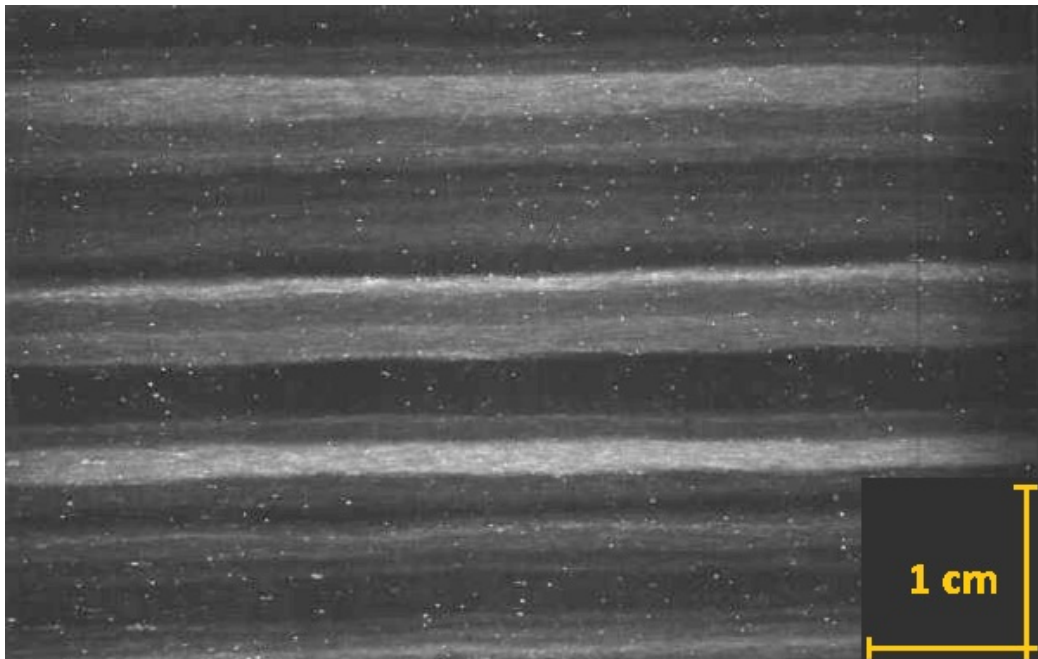
Figure 2.3: *Shows an example from bag 2727 (1500 m) which shows well layered cloudy bands.*

From the surface of the ice sheet until a depth of 1560 m we do not see any effect of shear stress which would cause folding in the parallel layered cloudy bands. With increasing depth the layering starts to get disturbed, and shows scattered folds. I considered the beginning of folding to occur in the bag which has three or more folds, which has been achieved in a depth of 1560 m.

2 Depth Region 2

As folding is just rarely obsereved in these depths, I considered this the transition zone between layering and folding. Occasionally there are anti- and synclinals in the layering (Fig. 2.4) and small Z-folds in thin layers (Fig. 2.6). Folding is not the dominant element of these dephts.
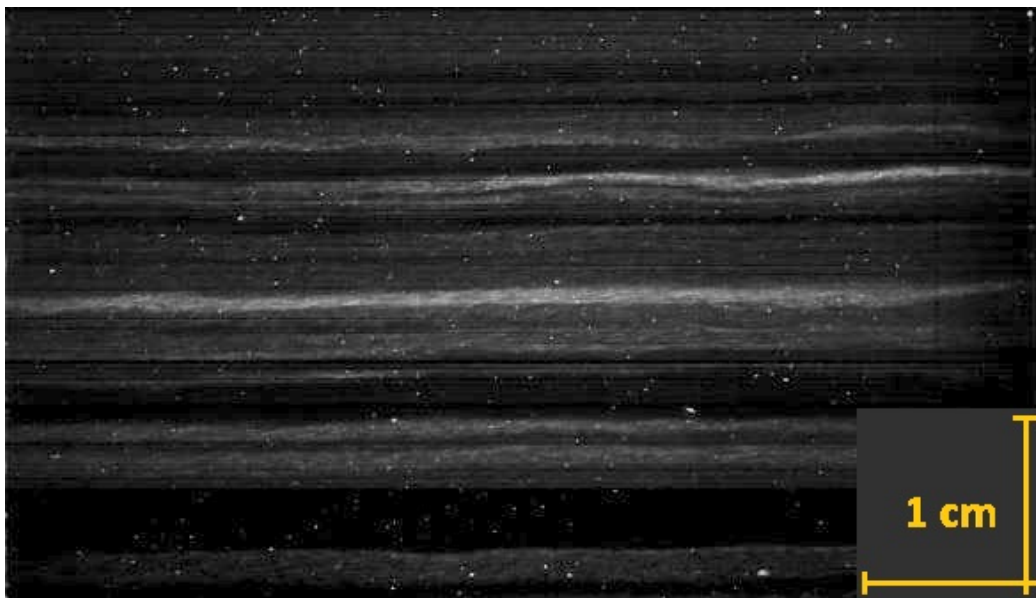
Figure 2.4: *Small waves in the layering (bag 2850; 1568 m).*

Fig. 2.4 shows a well layered set of cloudy bands with small waves. This is a typical image of the depth between layerd and folded cloudy bands. These waves increase in amplitude with depth, leading to folds.

11

Figure 2.5: *Small waves in the layering effecting several layers (bag 3159; 1738 m).*

Fig. 2.5 displays the evolution of shear zones in the layers. Two small steps in the cloudy bands lying on top of each other are visible. The top one is more dominant and more clearly evolved, the bottom one shows a small wave underneath the top one. The black layer inbetween follows the folding.
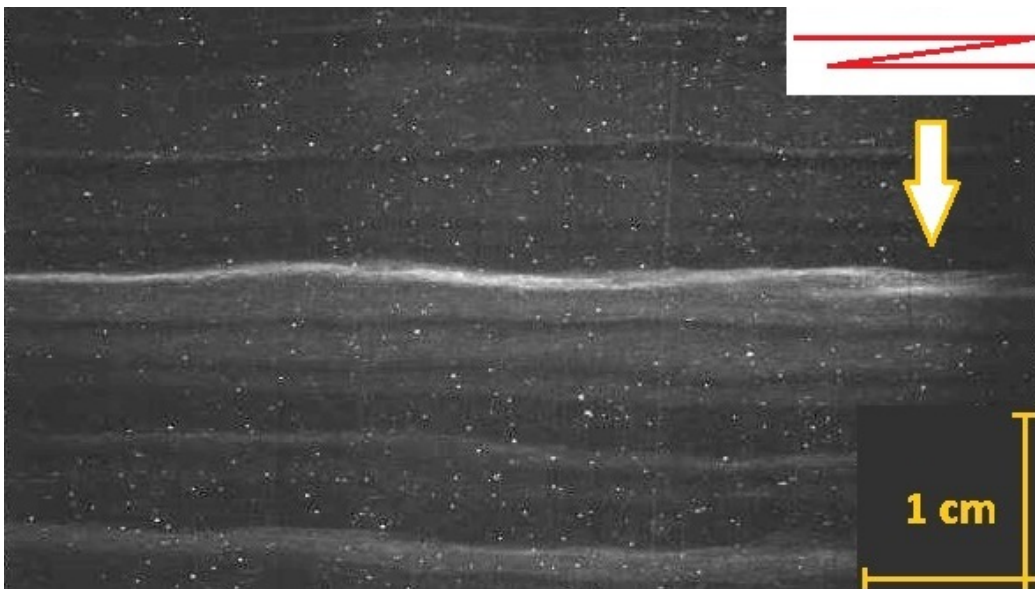
Figure 2.6: *Small Z-fold in a very thin layer (bag 3171; 1744 m). Including a sketch of the fold (red in white box)*

At the end of this transition zone there are small layers with Z-folds, as seen in fig. 2.6 This fold has no effect on the layers above and below, they are not disturbed by the Z-fold and well stratigrifyed. These types of folds become more common and affect the layers next to them, so I considered this part of the core to be the end of the transition zone. Addional folding itself becomes more common in the following bags.

3 Depth Region 3

The following 400 m of NEEM show folding, starting with asymmetric normal folds visible in the well layered cloudy bands, over layers with more than one fold and two folding events in one layer, until the shear rate is so high that it is no longer possible to describe each fold.
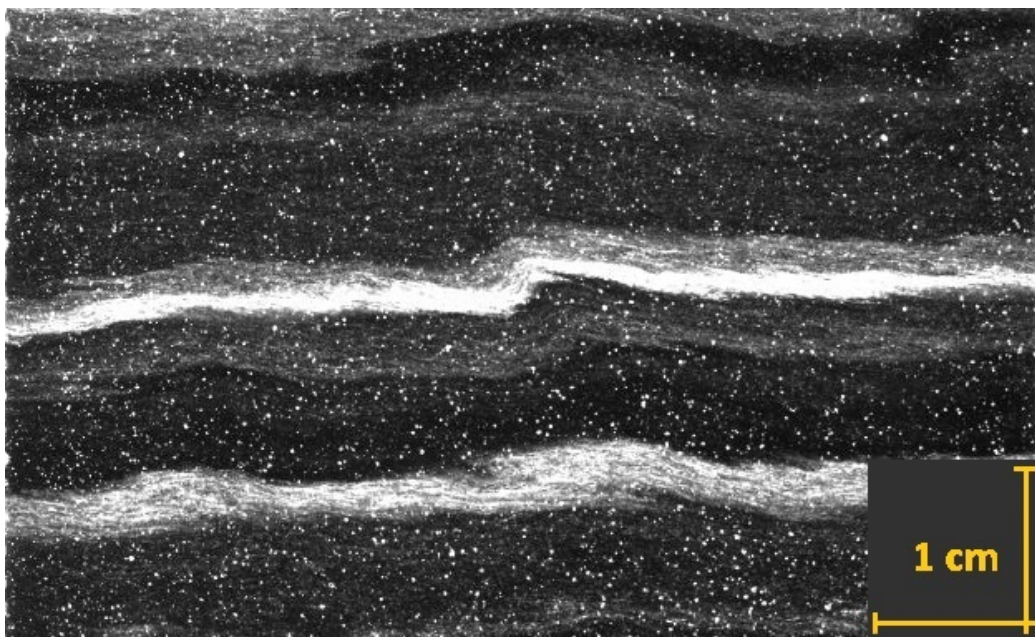
Figure 2.7: *Distinct, asymmetric fold (bag 3200 at 14 cm; 1760 m).*

The very bright cloudy band at 14.5 cm (Fig. 2.7) shows a very distinct fold. This is no symmetric anticline, as the left and right fold limb have different angles. Consequently, the fold axis which is located on the angle bisector of the fold limbs is tilted. With an angle of 15 ° from the vertical it creates a fold titled as Z-fold. The cloudy bands above and below show the same fold morphology. The top most and bottom most layer show effects of strain.
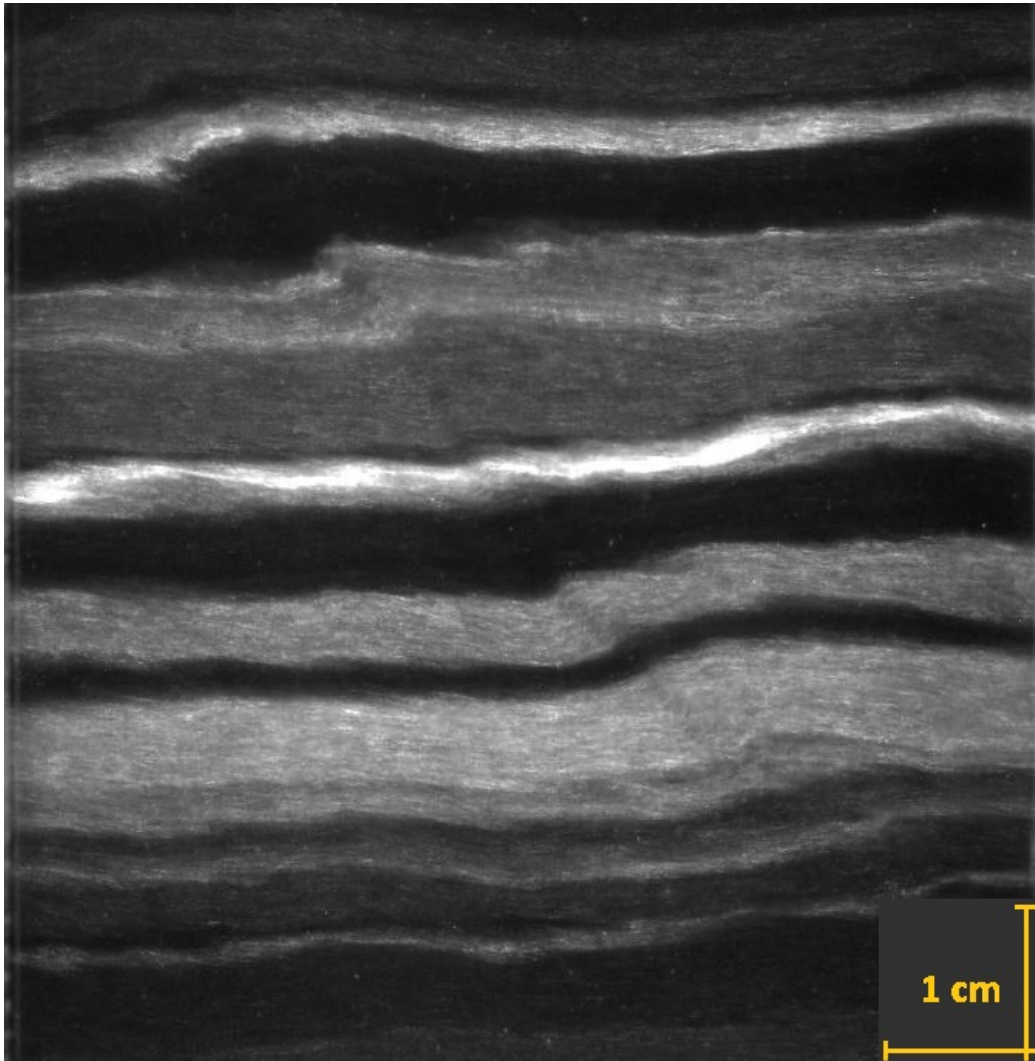
Figure 2.8: *Fold with a shear zone propagating below (bag 3202 at 25 cm; 1761 m).*

Folds at this depth affect the layers below as well. This is to be seen in the diagnonal line advancing through fig. 2.8 and disrupting the horizontal layering. This line causes Z-folds seen in the cloudy bands. The bright layer at 29.5 cm shows the highest effect of the shear zone, i.e. on top of this the shear stress has no effect. This is a typical type of fold and will become more frequent in greater depths.
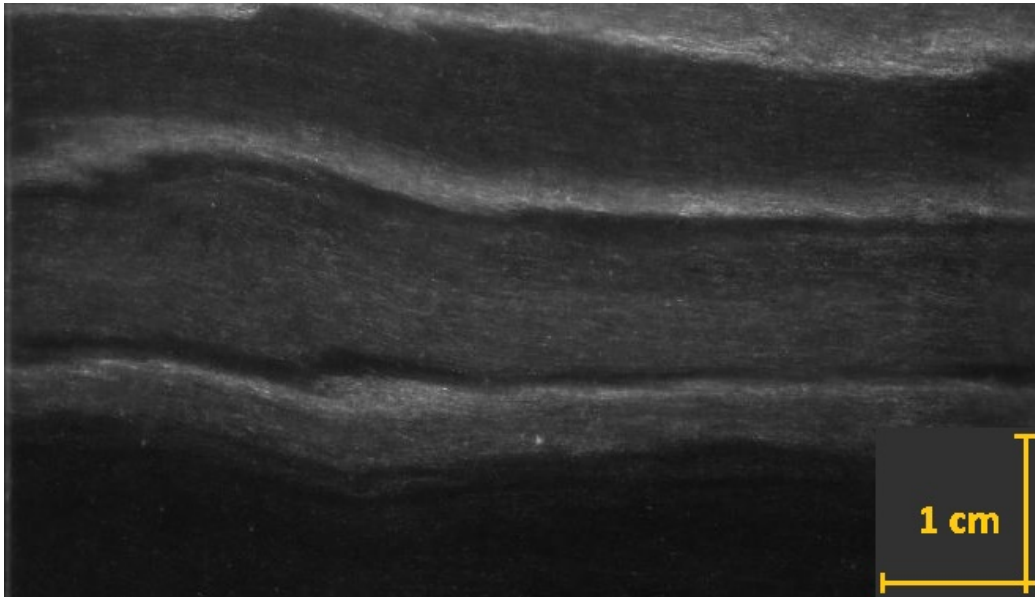
Figure 2.9: *Significant layer thickening (bag 3202 at 47 cm; 1761 m).*

On the small scale folding causes sinificant layer thickening (Fig. 2.9). From a thickness of 1.1 cm on the right there is an increase to 1.5 cm in the area of the folding. The effect of this on a small-scale isotope signal-measurement will be dicussed in the interpretation.
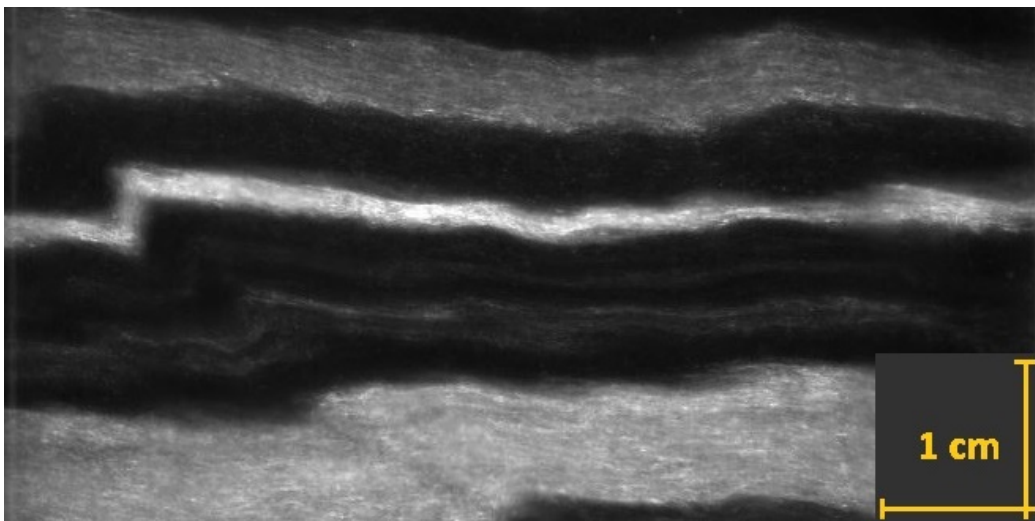
Figure 2.10: *Very angular fold hinge (bag 3204 at 77 cm; 1762 m).*

The bright layer in fig. 2.10 at 78 cm shows an angular fold hinge. This is a Z-fold and shows the different types of 'Z'-forms the layers can develop. At an angle of approximately 45 ° there is a shear zone propagating through the lower layers.
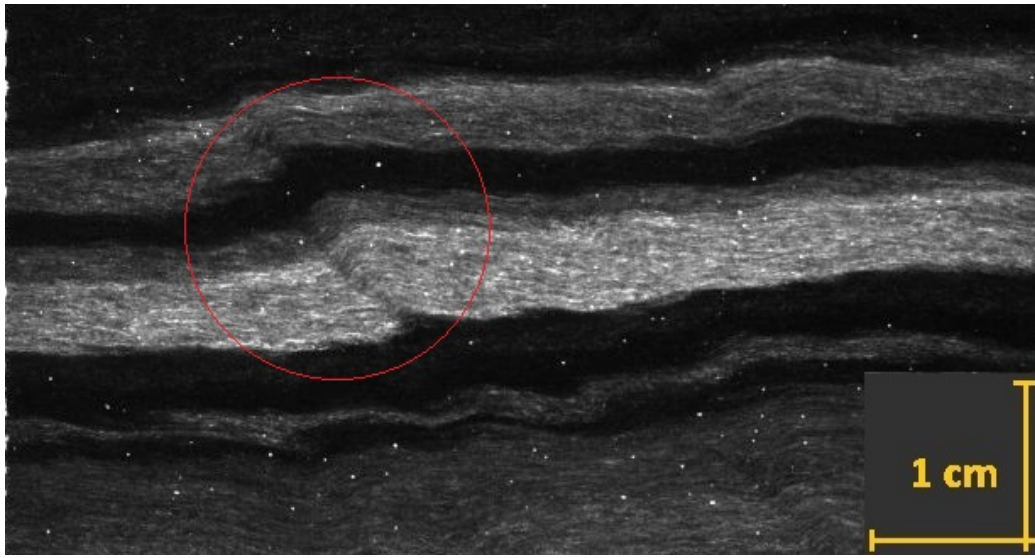
Figure 2.11: *Shear zone disrupting the layering (bag 3210 at 50 cm; 1765 m).*

This effect is rarely observed in cloudy bands. The top layer (Fig. 2.11) is affected by folding and lays at about 51 cm. Here we have a small wave, with smooth hinges not defined as a Z-fold. The gray layer beneath shows an overturned layer in the hinge of the fold. The black layer intrudes into the gray one. The fold at 50 cm shows a fold axis running through the layer and dragging the stratigraphy with it. There is no gap in the shear zone, but detachment of the layers, seen in a jump in the cloudy bands. In the interpretation this will be taken up again.

Note that there is a gap from 1765 m to 1823 m (bag 3210 to bag 3316). Due to few changes in the folding pattern I have skipped these meters. Now Z-folds are more stretched.
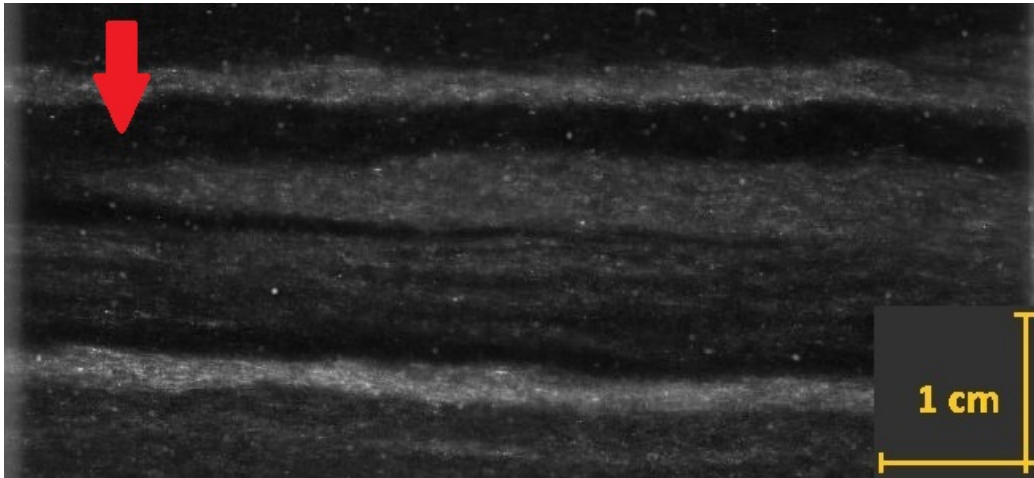
Figure 2.12: *Large Z-fold (bag 3316 at 29 cm; 1829 m).*

At 29 cm fig. 2.12 presents a layer that ends in a triangular form pointing to the left. This is a Z-fold with a bigger overthrust than the ones before. It is not clear how the layer continues outside of the core, but due to great overthrusting of this fold it is clear that this layer will appear twice in the record.
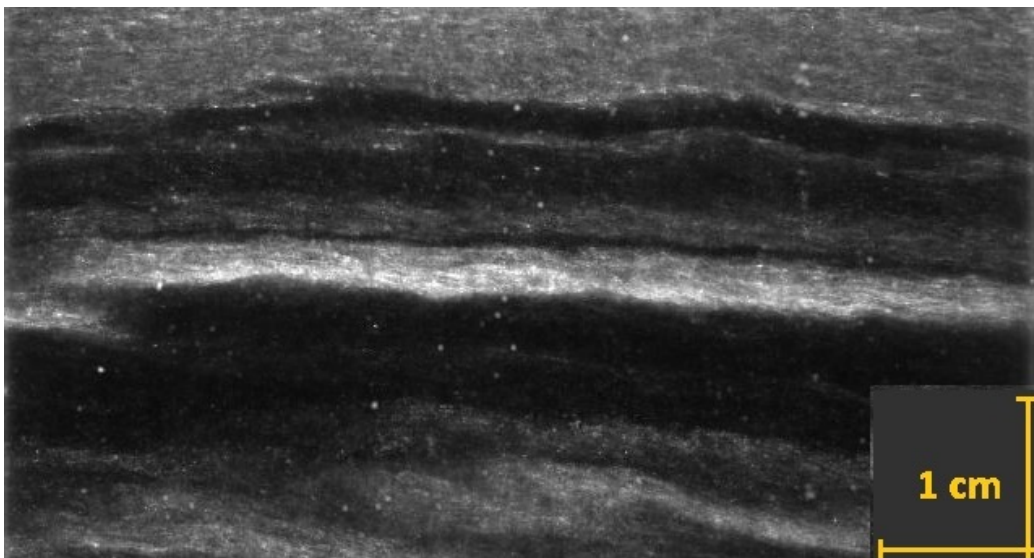
Figure 2.13: *Layer coming to a sudden stop at the left side of the picture (bag 3316 at 49 cm; 1829 m).*

Fig. 2.13 shows a bright layer at 49 cm, which suddenly stops at the left end

of the image and appears to go on several mm below. The Z-fold in the bottom leads to the assumption, that this is a shear zone separating this bright layer. This anomality will recieve more attention in the chapter "6 Outlook".
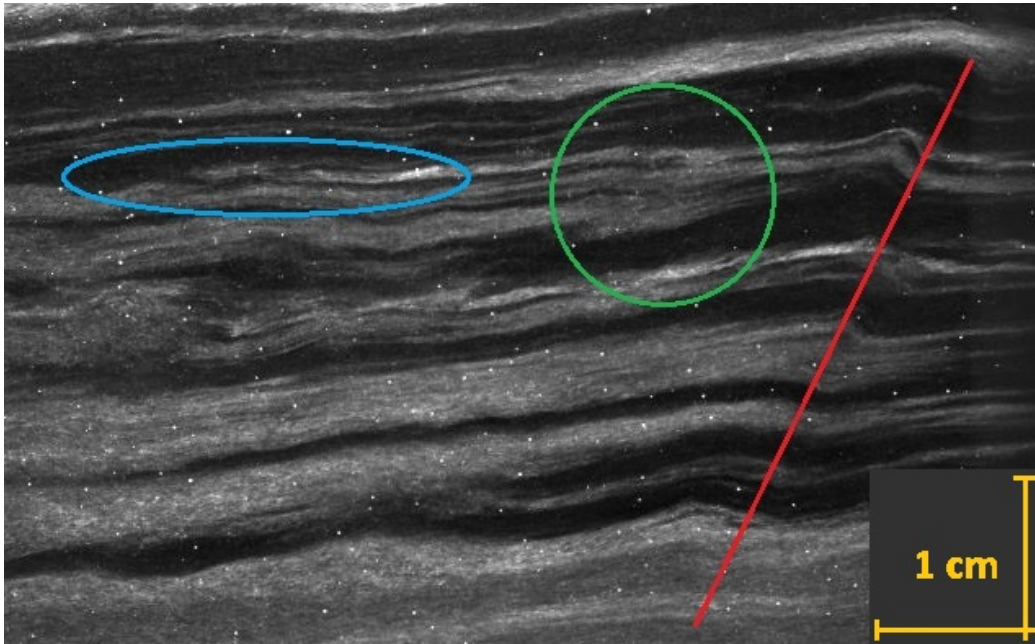
Figure 2.14: *Thin layers disturbed by a fold axis running through the right side of the image in red. Z-folds in green and layers that end in blue (bag 3596 at 26 cm; 1978 m).*

Fig. 2.14 shows the effect of a fold axis through many layers. Here we see thin layers that have been disturbed by a fold axis running through the side of the picture in a 65 ° angle (in red). This folding does not cause the overturning of layers, but a significant thickenning in the layers in the fold hinges. Additionally, some layers show Z-folds on a small scale which do not propagate far (green). The blue ellipse in the left of fig. 2.14 shows a thin layer that ends to the left. This is the effect of a long-streched Z-fold, which in this case is from an earlier deformation event. Due to this, this layer is a part of the folding event expressed by the red line.

Here again there is a gap (of 113 m) from 1977 m to 2090 m (bag 3596 to bag 3800).
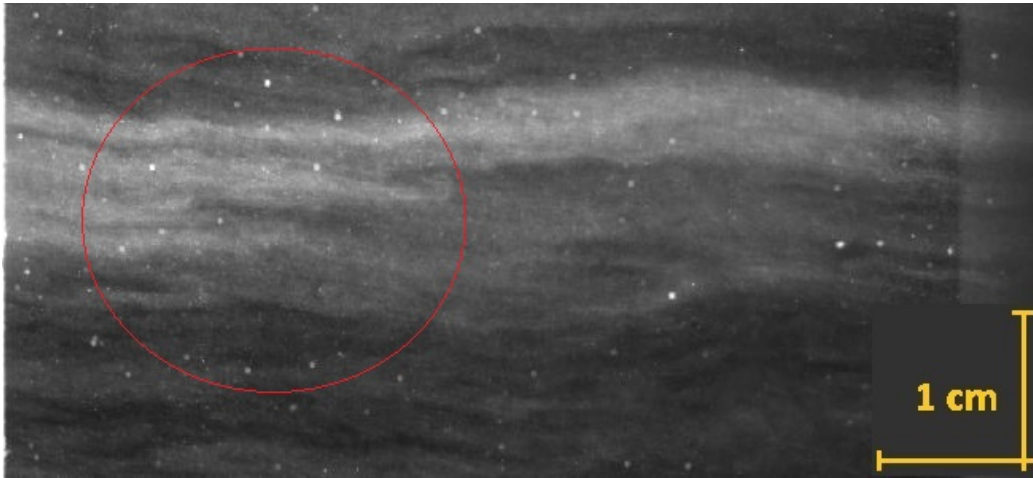
Figure 2.15: *Stack of Z-folds causing a significant thickening of the layer (bag 3800 at 90 cm; 2090 m).*

Fig. 2.15 does not anymore show stratific layering but instead a brighter layer which is continuous across the top and has at least two tight Z-folds at the left side. The darker layer follows the folding of the brighter one. The Z-folds on the left side lead to a thickening of the layer and a repetition of the layer from top to bottom.
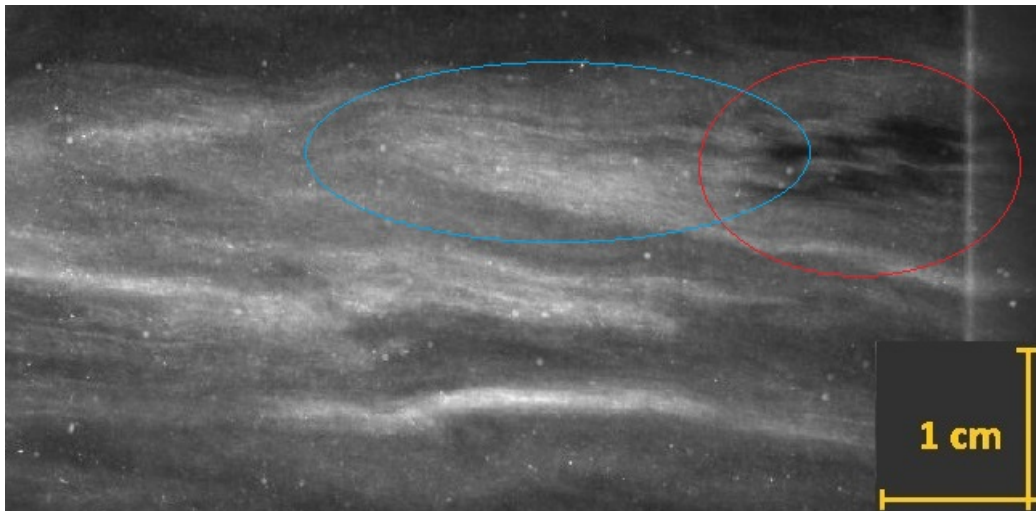
Figure 2.16: *Many types of folding in one area. Small Z-folds (red) and a large Z-fold (blue) (bag 3800 at 50 cm; 2090 m).*

At this depth more than one fold per layer can be observed. In fig. 2.16 there

are small Z-folds (red) on top of each other in the top right of the image and 2 cm farther to the left, at the same depth, a big Z-fold (blue).
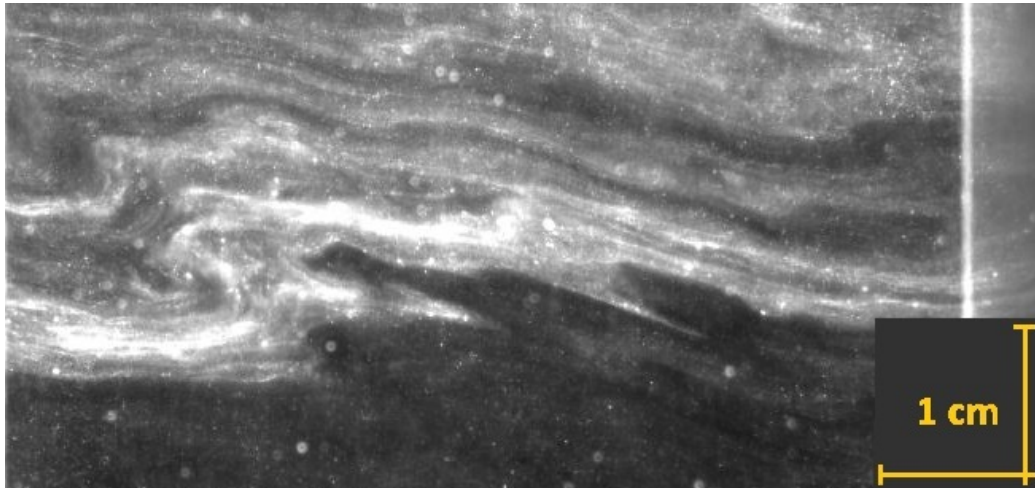
Figure 2.17: *Two Z-folds and stronly sheared layers (bag 2878 at 22 cm; 2132 m).*

Fig. 2.17 shows a bright layer which is folded several times and the fold hinges are strongly sheared out.
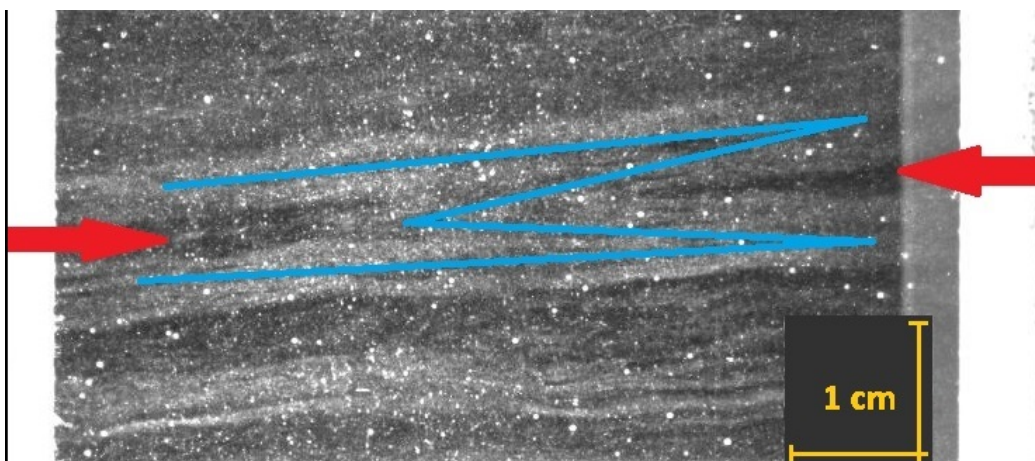
Figure 2.18: *Z-fold (blue), visible by dark layers ending (red arrows)(bag 3882 at 23 cm; 2135 m).*

Fig. 2.18 shows a Z-fold which is stretched across the entire scale of the im-

age. In blue are the layers, and the red arrows mark the dark layers that end in the hinges of the fold. This type of folding streches one layer several times across the image.
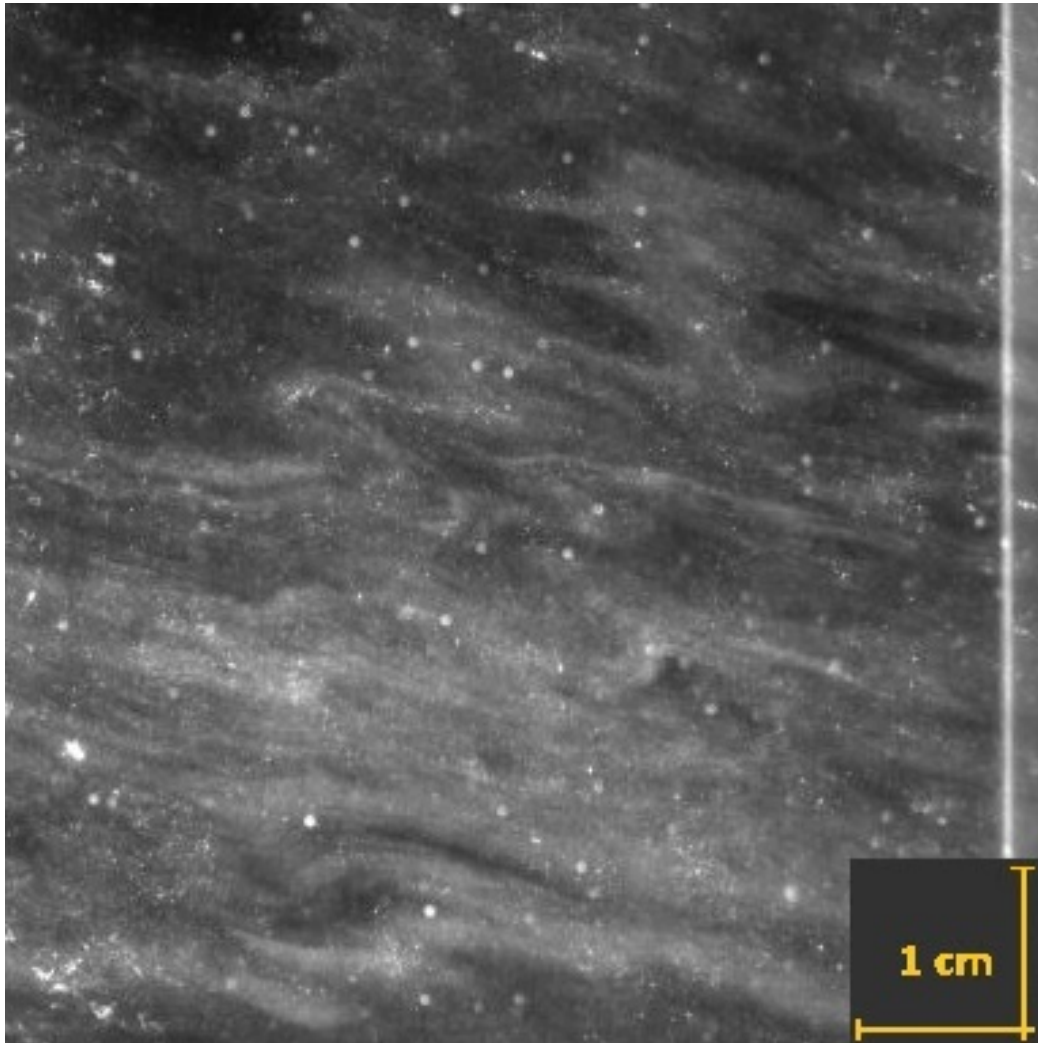
Figure 2.19: *Stack of Z-folds (bag 3908 at 25 cm; 2149 m).*

Fig. 2.19 shows a ca. 10 cm long excerpt of a core without layering. The dominant type of fold is Z-folding which causes great interruptions to the layering. E.g. the layer starting at 25 cm on the left side shows at least 5 Z-folds in the 8 cm cross-section of the core.
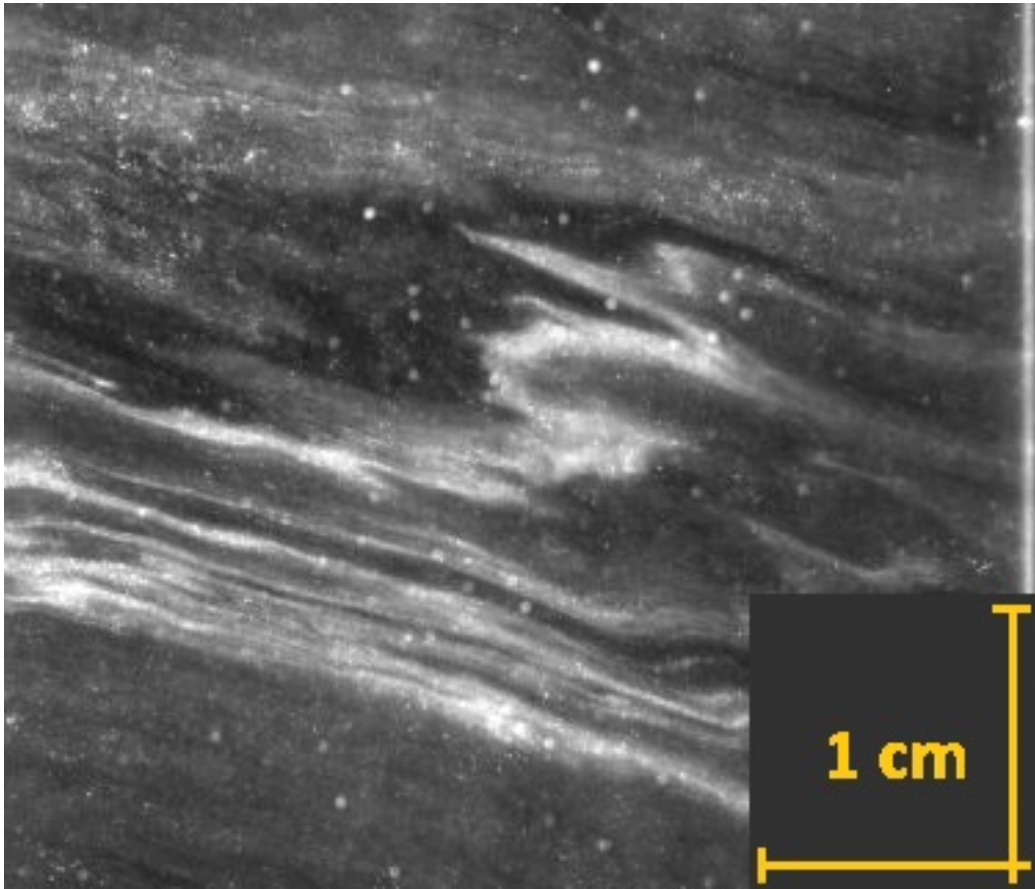
Figure 2.20: *Z-folds without classification scheme (bag 3909 at 15 cm; 2150 m).*

Fig. 2.19 shows roughly regular Z-folds, fig. 2.20 demonstrates irregularly sheared Z-folds. These fold hinges are streched out into other layers but the tracking of one cloudy band is possible through these folds.

4 Depth Region 4

From 2160 m (bag 3928) until the bottom of the core (2533 m; bag 4606) the stratigraphic layering becomes inconsistent. Cloudy bands are not visibile as layers, either because they are strongly sheared, or big crystals dominate at certain depths. At this depth (ca. 2200 m) the NEEM community (*NEEM community, 2013*) has tried to reconstruct a large scale fold. This was achieved with the duplication of the isotope signals. A recreating and revision of this theory is not possible with VS images.

At a depth of 2160 m small scale folding is very far advanced, resulting in strongly sheared layers.
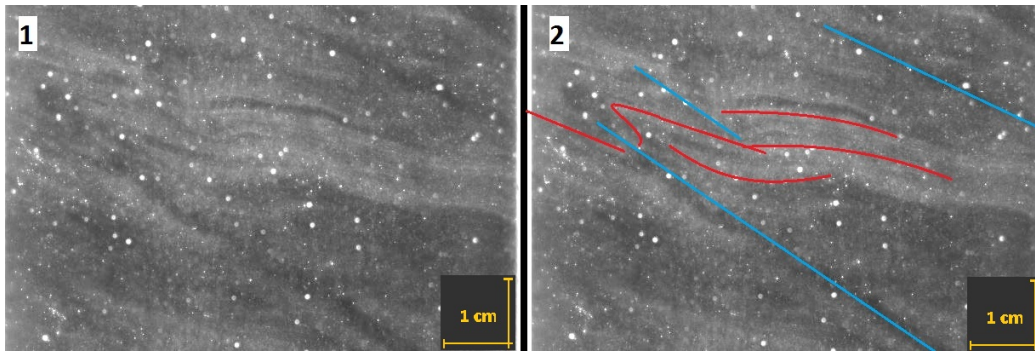
Figure 2.21: *Dark Eemian ice with shear zones (blue) and Z-folds (some in red, but most are not colored) (bag 3960; 2178 m).*

Reaching deaper into the core we outcrop ice from the Eemian warm period which is characteristicly more clear than ice from cold periods, and even with increased camera sensitivity the ice remains relativley dark. Yet it is possible to observe folding and shear zones. On the left side of fig. 2.21 we see a lot (5 to 7) of Z-folding and in the middle we can identify a shear zone.
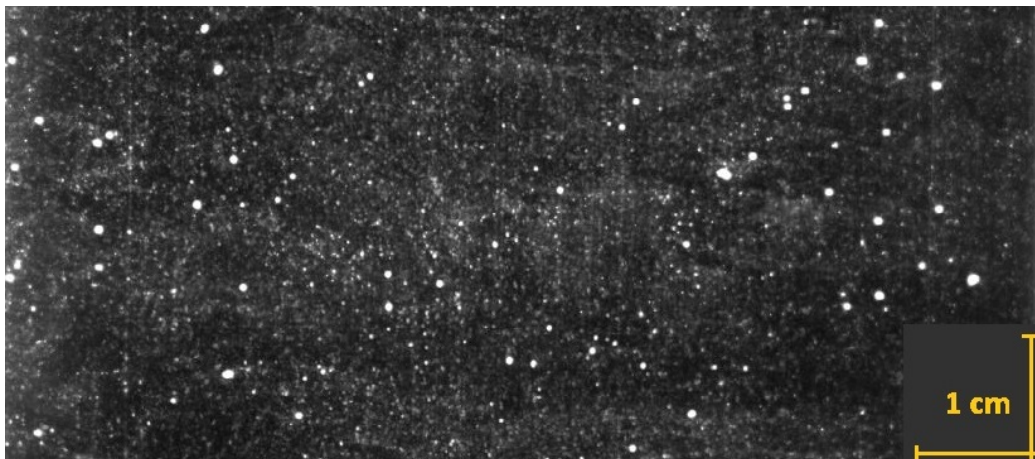
Figure 2.22: *Dark Eemian ice, where no more layering or cloudy bands are visible (bag 4000; 2200 m).*

Fig. 2.22 is an exemplary image which represents the ongoing structure of the

core. No layering is visible even with drastically increased camera sensitivity.

At depths close to the bottom of the ice sheet, the ice becomes brighter and shows cloudy bands of 50 cm thickness. This part is left out, as there is no more small scale folding here.

5 Similar Folds
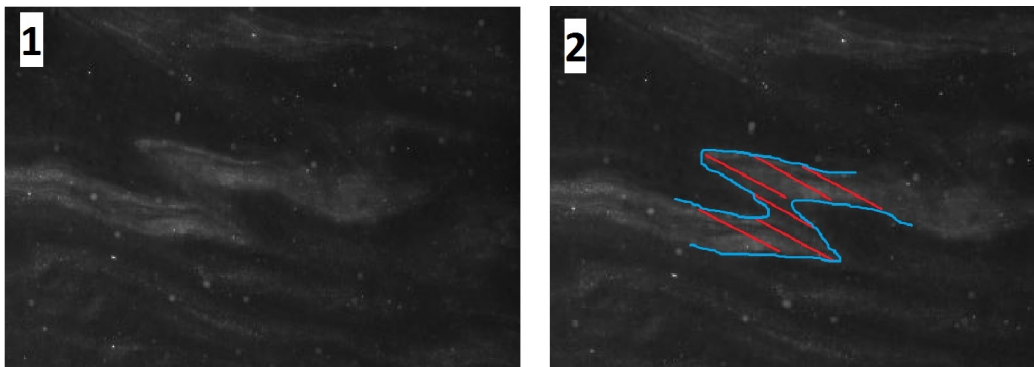
Figure 2.23: *Picture 1 and 2 show the same similar fold (bag 3750 at 09 cm; 2060 m), layer boundaries (blue) and the fold axis parallel thickness of the layer (red).*

As explained in chapter 1.4.2, similar folds are commonly observed in the cloudy bands. Fig. 2.23 shows an excerpt from bag 3750 (2060 m). The original image is displayed in fig. 2.23.1 and in fig. 2.23.2. I have sketched (in red) the thicknesses of the folded layer, parallel to the fold hinge. The layer boundaries are outlined in blue. This fold is clearly not symmetric but still displays the requirements for a similar fold.

2.3 Discussion
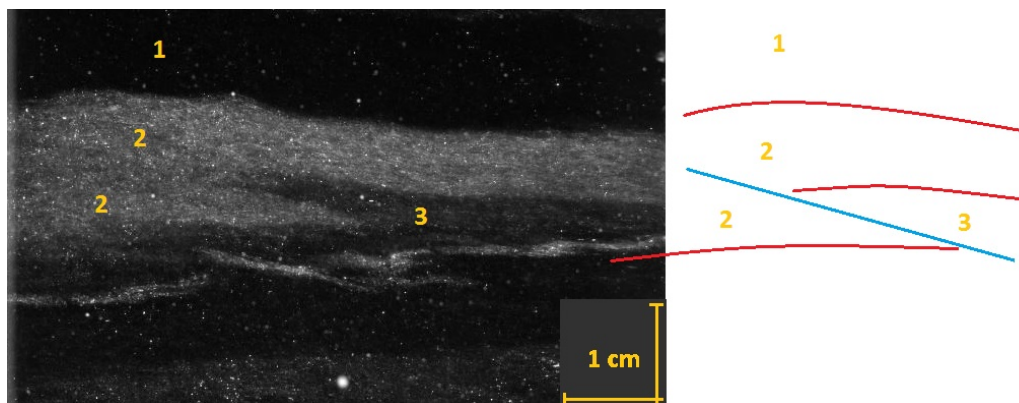
Figure 2.24: *Shows bag 3356 at 67 cm (1845 m) with shear zones (blue) and some layer boundaries (red)*

Double signal   Fig. 2.24 shows a significant thickening on the left side of the core, while the right side has the original thickness of the layer. Imagining this on a bigger scale, where the 8 cm of the core would be 80 m, we would receive different data from drillings on the left and and on the right side. In comparison to the right side, where we consider the signal undisturbed, the left side would show the signal twice, separated by a very thin layer reversed. This is the result of Z-folding in layers.

Data to core orientation   Throughout the core we have a dominant direction of the shear zones propagating from the top left to the bottom right of the picture. This changes in some parts, e.g. bag 3568 to bag 3638 or bag 3896, where it is from top right to bottom left. This is not in one exceptional fold but continues through many meters of the core. This could be explained easily by rotation of the core after drilling (which would be the simple explanation). A rather unlikely explanation would be change of flow direction of the glacier and therefore the change of strain direction, which would only seem probabale if we could determine the change of position of the ice divide.
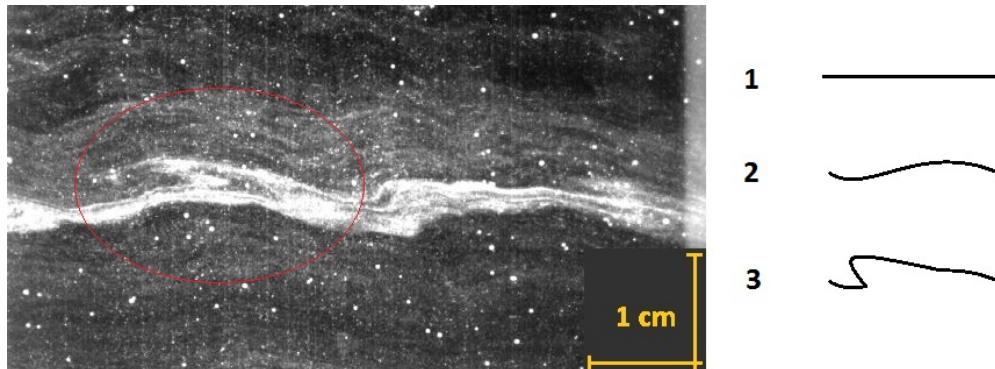
Figure 2.25: *Two folding events in one layer (bag 3890 at 35 cm; 2139 m). Sketched are the three steps of folding.*

Chronology of folds within one fold   Reaching 2160 m depth, we see many folds in one cloudy band. This gives the opportunity to reconstruct the order of folding. As in fig. 2.25 we have a thin cloudy band with two waves and a Z-fold in the middle. Additionally, we see that there is a dark part inserted inbetween the bright layers, which is the result of a folding event that happened later in time. The proof that it is the second event can be found in the fact that the Z-fold follows the waves of the layering.

Evolution of folds   Mentioned in depth region 3 (1560 m to 1750 m), fig. 2.5 shows two folds on top of each other. As it is obvious that they belong together, the black layer inbetween must also be part of the folding. This fold shows the start of folding, where adding strain will cause the layers above and below to also fold and later cause Z-folding, which evolves like the fold in fig. 2.8.

With increasing strain rate, we will encounter folds which look like those in fig. 2.13, where the hinges are strongly separated. With depth folding developes and we see one layer folded very often as in fig. 2.17. Reaching lower in the core we get folds shown in fig. 2.20 where very many folding events have taken place.

Having this at a depth far above 2200 m, we have to keep in mind that folding starts to occur at more shallow depths in ice than expected so far. It has to be considered if working with palaeo-climate records derived from ice cores or similar measurments in these areas, that realistic time sequence correlatation with other cores is ambiguous.

Offset along fold axes In fig. 2.11 (bag 3210 at 50 cm; 1765 m) the layering in the fold area shows an offset. Sticking to the idea that only ductil deformation can take place at this depth, we could consider the small hinge of the Z-fold to be so tight, that it is not possible to show this on the small scale and therefore it looks like it is not there.

Another possible explanation would be the combination of brittle and ductile deformation. The ductile component causing the bending of the layers to the shear zone and the brittle component causing the offset. As this effect can be observed in other folds too, it may be interesting to take a closer look at this in future works. (This will be presented again in the chapter "6 Outlook".)

Similar folds and not parallel folds Chapter "1.4.2 Measuring and plotting of Layer Thickness Variations" mentions the different types of folds, which are parallel and similar folds. Parallel folds are those created with a high competence contrast and maintain the same vertical thickness along the fold. They are the result of shearing and are suddenly created while the tension builds up reaching a certain threshold and then causes folding of the layer. These types are rarely observed in the available images of NEEM. The more common type is the similar fold which shows thinning in the fold limbs. This type (also called passive fold) is the consequence of insufficiant space, where layers of similar competences fold into each other.

As mentioned in chapter 1.4.3 it is possible to classify the type of folding using the plot in fig. 1.4. Most of the folds analyzed along the NEEM core will plot on the line of 'class 2, similar'. According to the schematics on the right side of fig. 1.4 one can see on first sight that this fits to most folds observed in NEEM.

Pure ductile deformation? Fig. 2.26 shows a folding example with several possibilities of interpretation. There is a dark zone (clear ice zone) in diagonal orientation in the figure, which separates the bright layer on the left from the one on the right. These seem to belong together, yet the one on the right side is significantly thinner. The edges of the layer, which are in direct contact to the zone in the middle are bent and it looks like they are bent down on both sides (Fig. 2.26). As a result of shearing, I would expect them to be bent oppositionally, i.e. one up and and the other one down, making them.
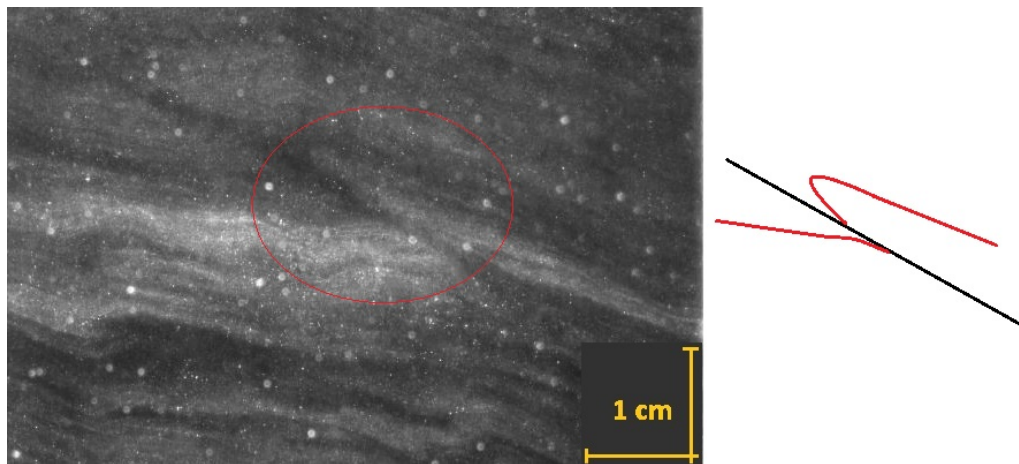
Figure 2.26: *Shear zone running diagonally through the image (bag 3912 at 6 cm; 2151 m). Shear zone sketched in black with one layer boundary in red.*

A possibility of interpretation would be that we have a fault running through the entire core, causing large scale brittle deformation. This is very unlikely at such a depth und and will not be further dicussed.
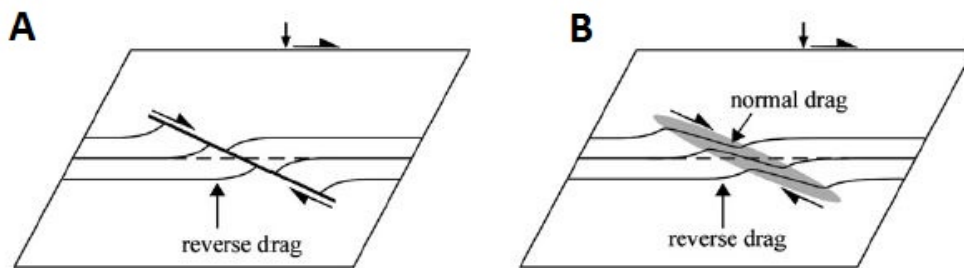
Figure 2.27: *Schematic reverse drag fold, showing the dragging of the layering along the shear zone. A is in a brittle environement, B in pure ductile deformation (modifyed from Gomez 2007).*

Another one would be a detachment fold, also known as drag fold. This type of fold is a mixture of brittle and ductil deformation. This results from a shear event where the fold hinges are dragged away from each other, which is explained in detail in Gomez (*Gomez, 2007*). The hinges are either dragged up or down and there is a main direction of the shear zone. Fig. 2.27 shows a drag fold in brittle (A) and ductile (B) shaping. The type observed in fig. 2.26 is a mixture of these two environments causing a brittle-ductile fold type.

What is also noticable in this image, is the very dark color of the shear zone. This will be discussed in the next paragraph.

New Ice in Shear Zones   Clear ice creates a dark coloring in the VS-images, due to missing scatterers (air bubbles, impurities, grain boundaries, etc.) in the dark field method. If some kind of recrystalisation during the shear event takes place, causing material to gather which has a different impurity load than the surrounding ice. Assuming that brittle-ductile deformation is possible, this will be a zone of strain localization up to faulting, where ice is transfered inside the zone of deformation that has a different particle composition than the surrounding ice. This transport may be enabled by diffusion in an under-pressure sourrounding, where a void tries to open but is unable to.

The zones of new ice and drag folds will be analyzed in the next chapter using the fabric images which give the orientation of the c-axis inside the core.

Chapter 3

c-Axis

3.1 Method: c-Axis Measurements
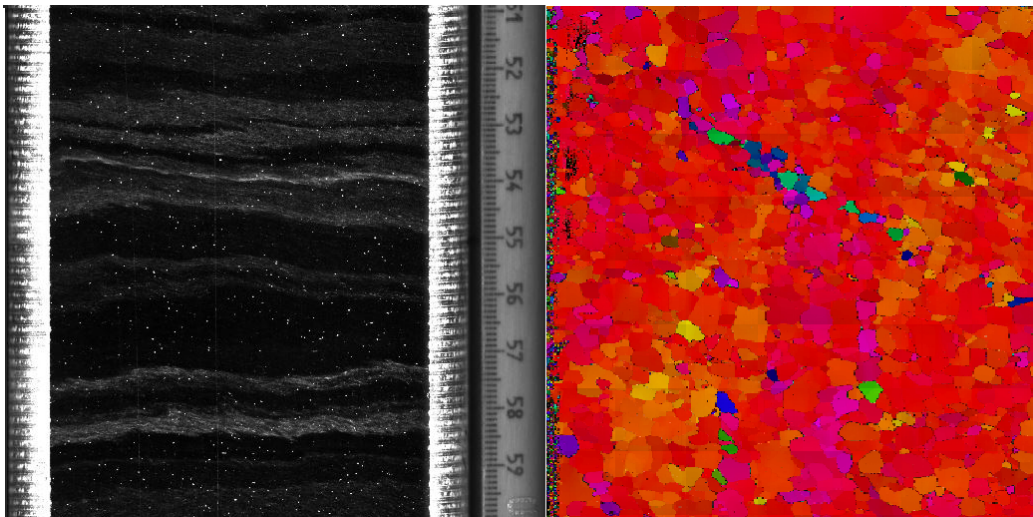
Figure 3.1: *Left: VS; right: fabric analysis (bag 3276 at 50 cm; 1801 m).*

As a basis for this chapter I refer to Surma (*Surma, 2011*), who gives an interpretation throughout NEEM with the c-axis orientation and Eichler (*Eichler, 2013*), wo created a program for automatic grain orientation detection. The data was mostly obtained directly in the field, where aproximately every 10 m one bag has been analyzed (*Montagnat, 2014*). This gives a record througout the core and shows the change of c-axis orientation. From the depth of 1750 m to 2150 m I have chosen 9 pictures with shear zones to analyze the orientation of the grains in the shear zones, from which I will discuss one in detail in this chapter.

Again I would like to thank the 'NEEM physical properties comunity' for giving me the full access to this data which is stored in 'Pangaea' (*www.pangaea.de*) and published by Prof Dr Ilka Weikusat and Dr Josef Kipfstuhl (*Weikusat, 2010*).

To display the orientation of the c-axis I used the 'Inverstigator' which is provided with the Fabric Analyzer Machine. If comparing to the VS method ('new camera system'), it has to be noted that the images must be turned as they are saved with the top to the bottom.

3.2 Results: Grain Orientation in Shear Zones

The images presented here have been created with *Investigator* and the freeware *Stereonet*. I have chosen one typical example from my analysis, and one more is displayed in the appendix, and shows similar orientations. The list of data points and all images are additionally on a DVD, which is part of this thesis.
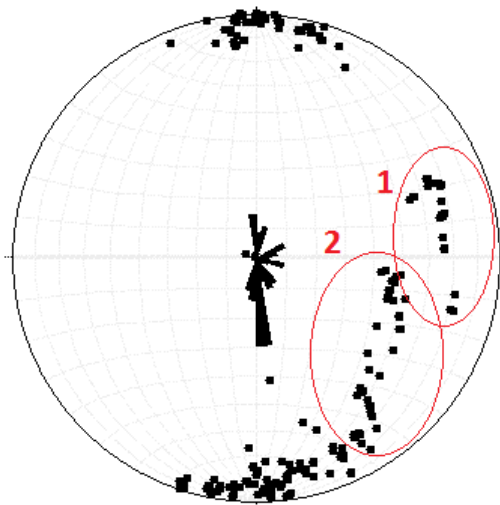
Figure 3.2: *Stereographic plot of c-axis orientation along a shear zone (bag 3276 at 50cm; 1801 m). Marked with red circles are the clusters 1 and 2.*

With increasing depth the grains undergo a reorientation. There is no preferred orientation of the c-axis in shallow depths, where the trend images of the fabric analysis shows no dominant color. They mainly have the color red, but also purple and yellow for grains with a c-axis orientation perpendicular in the core. Grains appearing in different colors than reddish have a different orientation from vertical. For increasing depth, the c-axes reorientate to a 90 ° to the ice sheet as well as the bed rock.

In a depth below 1500 m images appear mainly red and the c-axis orientation plots in the top and bottom ends of the stereonet, if the projection plane is chosen being the section plane of the vertical thin sections. Some however show more

31

or less straight lines of differently oriented grains running diagonally through the picture. Such an example can be seen in fig. 3.1 where c-axis and VS image are equally oriented with respect to the core axis (vertical direction in image).

I have randomly put approximetly 200 data points along the shear zone, to find its internal orientation (Fig. 3.2). Afterwards I have removed those on grain boundaries and grains which were not well analyzed. Those appearing in the top and bottom of the stereonet have a c-axis orientation perpendicular to the surface and the remaining ones are spread as a belt around the right side. For better overview a rose diagram as relative histogram in the center shows the main orientations.
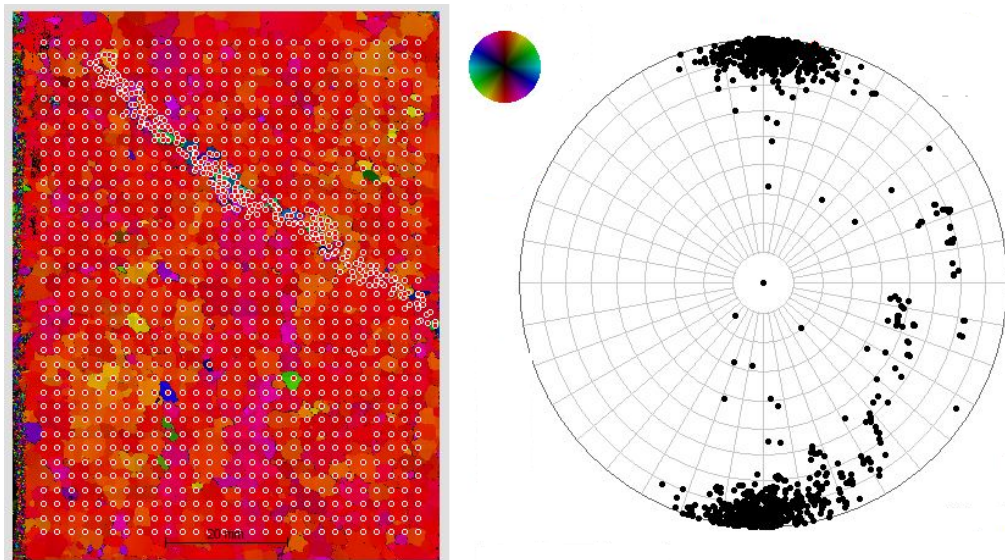
Figure 3.3: *Image from Inverstigator with all data points and the resulting stereoplot (bag 3276 at 50cm; 1801 m).*

Grid data evenly distributed across the entire sample and reduced by low-quality points show the average orientation (Fig. 3.3). The main clustering of these approximately 1000 points lays in the top and bottom. The measurement points on the shear zone again plot on the right side and are shown in the same plot as the 200 points from the shear zone.

3.3 Discussion

Shear zones do not create a random pattern in the c-axis distribution. There is a systematic scattering of these points as shown in fig. 3.2; this is along the bottom right (Cluster 1 and 2) side of the plot. I will name some possibilities to explain these plots.

First, some c-axes are oriented parallel to the shear zone. Considering this to be ductile with a considerable brittle component, c-axis parallel to the shear zone means basal planes perpendicular to this, which would not be a good prerequisite for sliding. There is another cluster higher on the right side (Cluster 1), which make a $40\,^\circ$ to $65\,^\circ$ angle to the shear zone which dips $130\,^\circ$ from the top. These basal planes do not show the orientation in which sliding would be possible.

The second idea is that the main factor of deformation at this depth is ductile. Therefore the possible evolution of the observed c-axes pattern is created by pure ductile deformation. Fig. 3.4 sketches the c-axis orientaion with perfect tilting in a Z-fold.

A perfect tilting of the c-axis would result in an orientation of $210\,^\circ$ which does not correlate with the results of the measurements.

Third, not all data points plot on one cluster, but form a belt around the right side of the steronet. The folding is the effect of simple shear which is sketched in fig. 3.5. Simple shear and thus the rotation of the c-axis create the observed orientation of grain in the fabric analysis image, where the shear zones are visible as a result of different c-axis orientation.

Another important consequence derived from these results is that measuring the mean crystal orientation throughout the core, the shear zone will disrupt the statistic averages.

Figure 3.4: *Perfect tilting of c-axis (in red) in a Z-fold.*
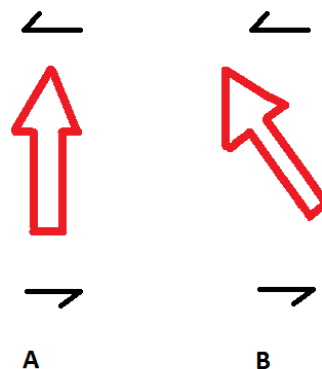
Figure 3.5: *Tilting of c-axis (in red) in simple shear.*

Chapter 4

3D-Orientation of Folds

4.1   Method: Visual Stratigraphy
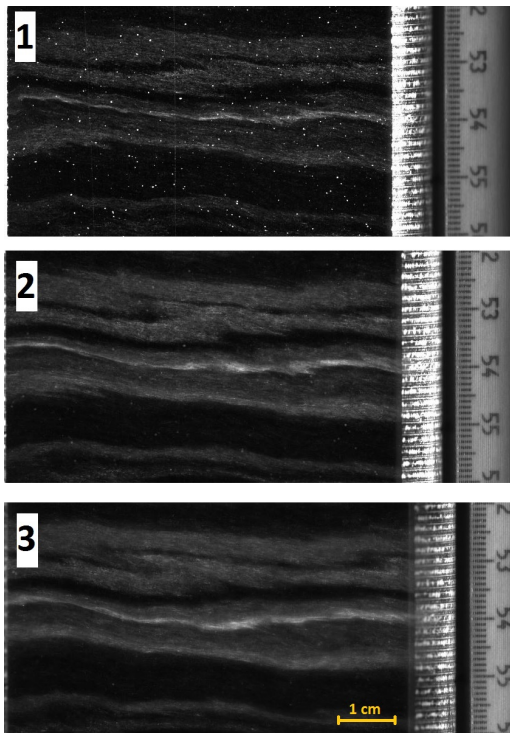
The VS images of each bag are taken at different focus levels. 'Pass 1' is 4 mm, 'Pass 2' 11 mm and 'Pass 3' is 18 mm below the cut and polishing surface. Within these 14 mm it is possible to define the exact direction of the fold axial plane. Fig. 4.1 shows the same fold as described in chapter "3 c-Axis".

Figure 4.1: *Bag 3276 (1801 m) at 3 different focus levels: -4 mm, -11 mm and -18 mm.*

4.2 Results: Shear Zone Orientation
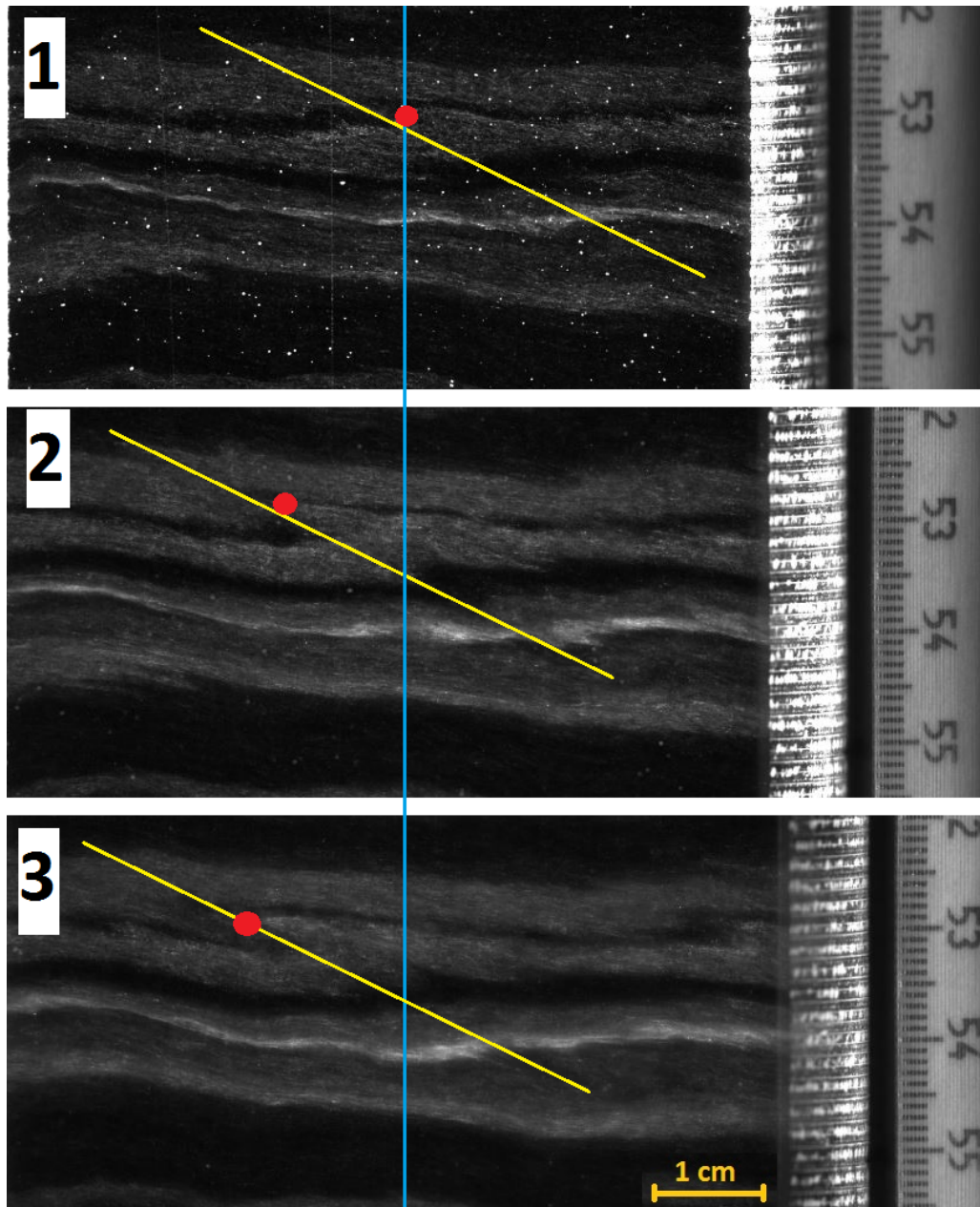
Figure 4.2: *Bag 3276 (1801 m) at focus levels -4 mm, -11 mm and -18 mm; with the fold axis (yellow), a guide line (blue) and the hinge (red).*

At a depth of 1801 m this Z-fold shows a shifting to the left as the camera focuses deeper. I have added a blue vertical line as a guide line for the eye,

from which the yellow line, which represents the fold axis, and the red dot, the fold hinge, move away with deeper focus. The angle of the fold axis shows no difference through fig. 4.2.1 to 4.2.3.
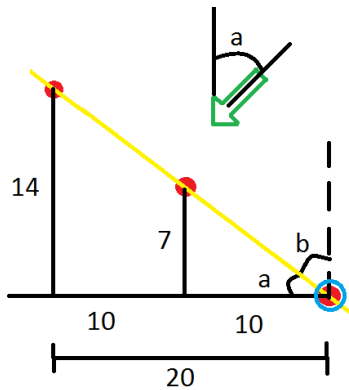
Figure 4.3: *Sketch of the fold from fig. 4.2, viewed from top; all values in [mm]; green arrow shows the main shear stress.*

Viewed from the top the fold plane can be shown as a line (yellow). The red dots are the same as in fig 4.2 and 7 and 14 are the vaules in [mm] of the different focus depths. 10 and 10 are an estimation of the vertical distance of these points. a is an angle of approximately $35°$ which can be calculated with cosinus $tan(a) = 14/20$.

b is $90° - a = 55°$. The main component of the shear stress is the green arrow which is $a = 35°$ to the right from a vertical view into the VS image. This goes hand in hand with the assumption and simplification, that the fold axial plane is perpendicular to the main shear stress.

4.3   Discussion

The main shear stress is in an angle to the VS image. This is not to be seen by analysing one 'pass' of the VS but needs the comparison of at least two focus levels. In the Excel sheet in the appendix (Table 8.1) I have given a general orientation of the shear zones which is either 'right' or 'left'. These informations only give a general idea of the fold orientation and are not sufficient for detailed analysis.

Chapter 5

Summary

Chapter 2 shows a detailed evolution of folding, illustrated with VS images at important depths, and presents ideas and explanatitions of folding evolution. Chapter 3 describes in detail one fold and gives information about the c-axis orientations with which shear zones can be identified. Chapter 4 gives an approach to the construction of the main shear stress. Combining all of these with the table (Table 8.1) given in the appendix, gives a record throughout the core referring to the small scale folding.

The argument of anisotropie of ice is often mentioned to explain the high compentence contrast, but not having parallel or buckle folds leaves this argument out. Also the modeling of high compentences shows different types of folds as the ones seen in NEEM. This can be evaluated in comparison with numerical models presented by Llorens (*Llorens, 2012*). An example of a similar fold is presented in chapter "2.3.5 Similar Fold" (Fig. 2.23) and can also be seen in other images shown in chapter "2 Folds in Ice".

The strain rate rises with increasing depth and shows influences in the layering at depths of 1500 m. The increase of shearing causes the cloudy bands to become unrecocnizable at depths below 2160 m. Here the VS is not useful anymore and other methods must be applied.

Chapter 6

Outlook

During my work with the VS images and fabric analysis on NEEM some questions have come up.

In bag 3896 (2142 m) there are some folds with shear zones running through them. These zones are very dark, i.e. filled with very clear ice. I have mentioned this in chapter "2.3 Discussion" but this occurence needs more attention. Two of these examples are fig. 3.3 and 8.1 in the appendix.

Fig. 2.13 shows a layer that ends suddenly and may be the result of brittle behavior. As this occures often, another explanation than pure ductile deformation in the ice sheet is worth being thought about.

The research of internal deformation and flow of salt is starting to become interesting for geologists. As ice and salt have similar physical properties and the small scale folding looks alike, the cooperation of ice glacier deformation and salt glacier deformation research may be of use for both sides. Fig. 8.3 shows an image from a wall in an abandond salt mine in Russia.

Chapter 7

References

Benn, D., Evans, D. 2010. *Glaciers and Glaciation.* Hodder Arnold Publication. ISBN-13: 978-0340905791.

Daily mail, *article-2552245-1B35FE6100000578-970_964x642.jpg,* available online at
http://www.dailymail.co.uk/news/article-2552245/The-psychedelic-salt-Abandoned-Russian-tunnels-mind-bending-patterns-naturally-cover-surface.html (access date: Mai 20th, 2014).

Davis, G., Reynolds, S., Kluth, C. 2011. *Structural Geology of Rocks and Regions.* Wiley; 3. edition. ISBN-13: 978-0471152316.

Eichler, J. 2013. *C-Axis Analysis of the NEEM Ice Core – An Approach based on Digital Image Processing,* Fachbereich Physik, Freie Universität Berlin, 2013, http://epic.awi.de/33070/.

Faria, S., Freitag, J., Kipfstuhl, S. 2010. Polar ice structure and the integrity of ice-core paleoclimate records. *Quaternary Science Reviews* **29**, 338–351.

Gomez-Rivas, E., Bons, P., Griera, A., Carreras, J., Druguet, E., Evans, L. 2007. Strain and vorticity analysis using small-scale faults and associated drag folds. *Journal of Structural Geology,* **29** 1882-1899.

Hall, Sir J. 1815. II. On the Vertical Position and Convolutions of certain Strata, and their relation with Granite. *Earth and Environmental Science Transactions of the Royal Society of Edinburgh* **7**, Issue 01, 79-108. Doi: 10.1017/S0080456800019268. Published online by Cambridge University Press January 17th, 2013.

Kipfstuhl, J. 2010. Visual stratigraphy of the NEEM ice core with a line-scanner. *Alfred-Wegener-Institute, Helmholtz-Center for Polar and Marine-Research, Bremerhaven,* Unpublished dataset Nr. 743062.

Kuhs, W. 2007. *Physics and Chemistry of Ice.* RSC Publishing, London. ISBN-13: 978-0854043507.

Llorens, M.-G., Bons, P., Griera, A., Gomez-Rivas, E., a, Evans, L. 2012. Single layer folding in simple shear. *Journal of Structural Geology.* Doi:10.1016/j.jsg.2012.04.002.

Montagnat, M., Azuma, N., Dahl-Jensen, D., Eichler, J., Fujita, S., Gillet-Chaulet, F., Kipfstuhl, S., Samyn, D., Svensson, A., and Weikusat, I. 2014. Fabric along the NEEM ice core, Greenland, and its comparison with GRIP and NGRIP ice cores, *The Cryosphere*, **8**, 1129–1138.

NEEM homepage, *Greenland.bmp*, available online at http://neem.dk/neeminfo.pdf (access date: July 5th, 2014).

NEEM community. 2013. Eemian interglacial reconstructed from a Greenland folded ice core. *Nature* **493**, 489-494.

Ram, M., Koenig, G. 1997. Continuous dust concentration profile of pre-Holocene ice from the Greenland Ice Sheet Project 2 ice core: Dust stadials, interstadials, and the Eemian. *Journal of Geophysical Research: Oceans (1978–2012)* **102**, Issue C12, 26641–26648. Doi: 10.1029/96JC03548.

Ramsay, J., Huber, M. 1987. *The Techniques of Modern Structural Geology: Folds and Fractures.* Academic Press; 1. edition. ISBN-13: 978-0125769228.

Schmalholz, S., Fletcher, R. 2011. The exponential flow law applied to necking and folding of a ductile layer. *Geophysical Journal International* **184**, 83–89. Doi: 10.1111/j.1365-246X.2010.04846.x.

Svensson, A., Nielsen, S., Kipfstuhl, S., Johnsen, S., Steffensen, J., Bigler, M., Ruth, U., Röthlisberger, R. 2004. Visual stratigraphy of the North Greenland Ice Core Project (NorthGRIP) ice core during the last glacial period. *Journal of Geophysical Research* **110**. Doi: 10.1029/2004JD005134.

Surma, J. 2011. *Die Orientierungen der C-Achsen im NEEM Eiskern (Grönland).* Institut für Geologie und Mineralogie, Universität zu Köln, http://epic.awi.de/26101/.

Thorsteinsson, T. 2000. *Anosotropy of ice I_h: Development of fabric and effects of anisotropy on deformation.* University of Washington.

Van Hise, C. 1896. Principles of North American Precambrian Geology. *U.S. Geological Survay Annual Reports* **16**, 581-843.

Weikusat, I., Kipfstuhl, J. 2010. Crystal c-axes (fabric) of ice core samples collected from the NEEM ice core. *Alfred Wegener Institute, Helmholtz Center for Polar and Marine Research, Bremerhaven,* Unpublished dataset #744004.

Chapter 8

Appendix

8.1   c-Axis, Second Example

In chapter "3 c-Axis", I have explained in detail an example of the grain orientation in shear zones. This section should shortly persent another example.
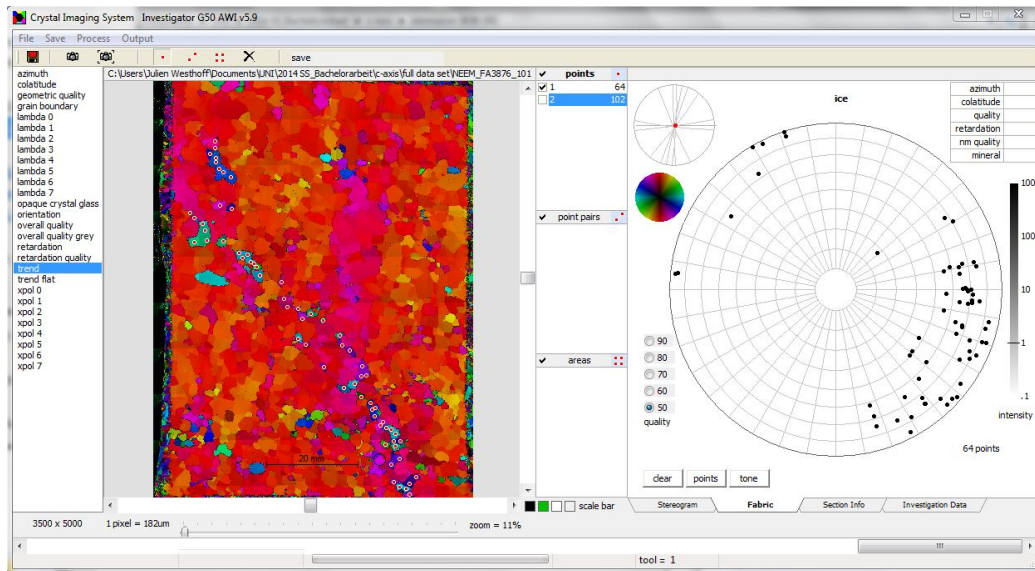
Figure 8.1: *Orientation of the c-axis (bag 3876 at 10 cm; 2131 m) with resulting stereoplot in the shear zone.*

Fig. 8.1 shows the orientation of the c-axis in bag 3876 at 10 cm. In this case I have only put points on the grains with a different orientation. These again all plot in a cluster in the bottom right to right area of the sterographic net.

As expected the remaining grains in this shear zone, i.e. the ones aligning with the ones ploted earlier (Fig. 3.3), plot in the top and bottom and have aproximetly the same orientation as the remaing grains.
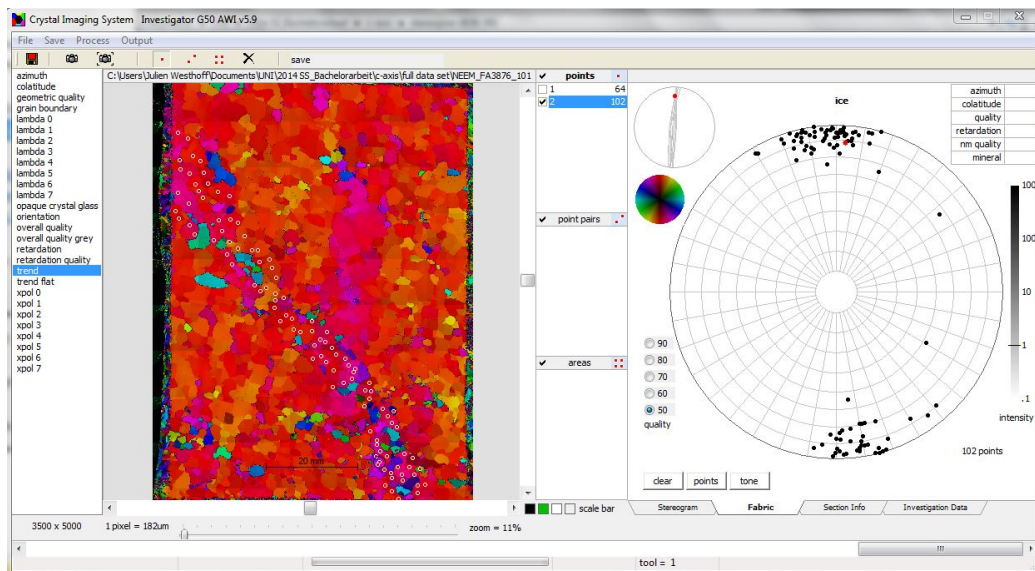
Figure 8.2: *Orientation of the c-axis (bag 3876 at 10 cm; 2131 m) with resulting stereoplot across the image.*

Adding to this the area across the whole section created a plot as seen before in chapter "3 c-Axis". The main direction of the c-axis orientation is parallel to the core and just the shhear zone shows differences from this.

8.2 Salt

Figure 8.3: *Wall of an abandoned salt mine in Russia (image from www.dailymail.co.uk).*

Fig. 8.3 shows a wall of an abandond salt mine in Russia. The folding structures are the same as in ice and is visible due to different colors in the layers of salt.

8.3 Excel Sheet

The following tabel shows the notes I made while examining the VS images of NEEM from top to bottom. The table is simplifyed to make it fit to the page. Shown here:

- bag number of the first bag of each data set (2 to 3 bags per file)

- the corresponding depth

- type of visible structure

- depth in cm in the bag correlating to the fold

- fold type

- estimate of the layer thickness containing the fold

- relative color (0=black, 10=white)

- number of folds in the layer

- fold axis orientation (left or right)

- a comment

For readebility reasons, please note, that the following items are missing in this paper print-out, but are available on the attached DVD:

- the number of the second bag, which would be the second column

- an estimation to the wave length

- the linescanner camera used (old or new)

- the image number and 'pass' used for the observation

- if the layer shows a significant thickening which is mostly due to folds laying ontop of each other

Bag	Depth	Structure	cm scale	Fold type	Thick-ness	Color	No. of Folds	Fold axis ori-ent.	Comment
2100	1.155,275	no layer-ing							
2727	1.500,125	horizontal							
2730		horizontal							
2733		horizontal							
2799		ca hori-zontal							
2802		ca hori-zontal							
2805		ca hori-zontal							
2850	1.567,775	small waves							folding starts
2853		small waves							folding starts
2856		small waves							folding starts

Bag	Depth	Structure	cm scale	Fold type	Thick-ness	Color	No. of Folds	Fold axis ori-ent.	Comment
2898		small waves							
2901		small waves							
2904		small waves							
2949		small folds	1/2	asymmetric fold					1 small asymmetric fold
2952		waves, small ampli-tude							
2955		small waves							
3000		small waves							
3003		small waves							
3006		small waves							
3009		small waves							

Bag	Depth	Structure	cm scale	Fold type	Thick-ness	Color	No. of Folds	Fold axis ori-ent.	Comment
3051		start of asym-metric fold	middle	asymmetric fold	10	all	1		
3054		small waves							small asymmetric fold
3057		small waves							4 small asymmet-ric folds
3099		layering							
3102		small waves							
3105		small waves							
3150		small waves							
3153		smal folds							low amplitude
3156		small waves							
3159		small waves							starting of prop. Faults

Bag	Depth	Structure	cm scale	Fold type	Thick-ness	Color	No. of Folds	Fold axis ori-ent.	Comment
3162		small waves	11	shearzone	40	all	1	right	
3165		small waves							
3168		small waves							
3171		small waves	80	thrust fault/fold	1	10	1		layer thickening
3174		small waves	40	shearzone					low amplitude, starting of prop. Faults
3177		small waves							
3180		small waves	100	thrust fault/fold	1	9	3		
3183	1.750,925	small waves							
3186		small waves							increasing ampli-tude
3189	1.754,225	folding	ca 80	Z	2	8	1		
			ca 10	asymmetric fold	1	9	2		
3192		folding	65	Z	1	8	1		

Bag	Depth	Structure	cm scale	Fold type	Thick-ness	Color	No. of Folds	Fold axis ori-ent.	Comment
3195		no layers visible							
3197		folding	49 top	Waves	2	7	5	left	right side 5mm higher than left.
			46,5	Normal	3	8	1		
			43	Waves	4	6	2		folds also 2 cm below
			35.5	asymmetric fold	3	8	2	left	
3198		horizontal							
3200		folding	100	large scale	10	8	0.5		right side higher than left
			88	large scale	5	8	1		
			54	Z	1	9	3	left	
			52	asymmetric fold	8	7	1	left	
			52	Z	3	9	1	left	
			31	Z	4				interesting
			14	Z	3	10	1	left	asymmetric fold
3202		folding	99	Z	1	9	3	left	
			47	shearzone	30	7	1	left	
			25	shearzone	55	all	1	left	

Bag	Depth	Structure	cm scale	Fold type	Thick-ness	Color	No. of Folds	Fold axis ori-ent.	Comment
			15	shearzone	40	all	1	left	
3204		folding	98	shearzone	40	all	2	left	large
			78 to 62	shearzone					one after another
			57	shearzone					angle of displace-ment gets smaller
			18	asymmetric fold			3	left	3 different angles of displacement line
3206	1.763,300	folding	87	shearzone		all	1	left	
			82	Z	3	1	1		
			74	asymmetric fold		all	1	left	
			50	Z	10	7	1	left	
			27 to 20	shearzone		all	2	left	
3208		folding	100	Z			many	left	many folds. C-axis could be in-teresting here
			84	shearzone	40	all	1	left	
			62	shearzone	40	all	2		2 faults with dif-feren angles
			24	?	5	0	many		
3210		folding	105	Z	10	8	4	left	
			83	Z	15	8	2	left	

Bag	Depth	Structure	cm scale	Fold type	Thick-ness	Color	No. of Folds	Fold axis ori-ent.	Comment
			80	asymmetric fold	25	all	3	left	
			50	thrust fold	10	8	1		thrust fold
			36 to 31	shearzone	50	all	1	left	
			24	Z	5	7	1		
			7	Z	3	7	1	left	
3212		folding	106	Z	15	all	1	left	
			99	Z	12	all	2	left	
			91	shearzone	30	all	2	left	
			79	thrust fold	10	8	1	left	
			59	Z	20	7	2	left	
			43	Waves		all	1	left	
			36	thrust fold	2	9	1		thrust fold ?
			31	asymmetric fold	10	7	1	left	
			25	Z	15		2	left	
			18	asymmetric fold	13	5	1	left	
			14	Z	10	6	2		
			3	all	20	all	1	left	

Bag	Depth	Structure	cm scale	Fold type	Thick- ness	Color	No. of Folds	Fold axis ori- ent.	Comment
3214		folding	117	asymmetric fold	15	all	1	left	
			92	thrust fault	3	6	1		thrust fault? Or fold?
			84	shearzone	25	all	1	left	
			74	asymmetric fold	50	all	1	left	
			70	shearzone	60	all	2	left	different angles
			48	normal fold	5	8	1		
			47	shearzone	25	all	1	left	Nice c-axis! Check 3D. Pass30=normal fold, pass10=prop.fault
			33	shearzone		all	2	left	
			3	shearzone	30	all	1	left	
3216		folding	110	Waves	9	1	3	left	
			91	Z	1	7	1		
			73	asymmetric fold	5	8	1	left	
			70	all	20	all	1		check c-axis; but no data
			44	shearzone	10	all	1	left	bent fold axis?

Bag	Depth	Structure	cm scale	Fold type	Thick-ness	Color	No. of Folds	Fold axis ori-ent.	Comment
			36	asymmetric fold	20	7	1	left	
			20 to 17	shearzone	40	all	2	left	
			12 , 5	Z	3	0	1		
3226		folding	96	waves	8	7	3	right	
			66	waves	35	all		right	
			56	shearzone	40	all	3	right	
			46	Z	2	7	1		
			25	waves	2	9	4	right	
			6	asymmetric fold	3	0	1		c-axis data but no match
3236	1.779,250	folding	115	shearzone	60	all	2	left	
			86	Z	5	0 and 7	2	left	very over tilted
			79	shearzone	15	all	1	left	
			71	Z	4	0	2		
			49	waves	8	5			
			38 , 5	Z	2	6	3	left	

Bag	Depth	Structure	cm scale	Fold type	Thick-ness	Color	No. of Folds	Fold axis ori-ent.	Comment
			28	waves	5	9		left	Z folds at top and bottom
			21	shearzone	20	7	1	left	okay match
			11	asymmetric fold	7	8	1		line on the very right
			5	shearzone	30	all	2	left	
3244	1.784,200	folding	107	shearzone	40	all	1	left	
			57	Z	5	3	1	left	
			55 , 5	Z	1	1	1	left	fold axis goes through black?
			53 to 50	shearzone	25	all	2	left	
3276		folding	107	shearzone	20	all	1	left	check c-axis at 50 and 60
			103	waves	15	all	2	left	
			98	Z	5	8	2	left	small Z folds throught core
			60	Z	1	8	5	left	
			53	Z	15	all	1	left	
			36 to 30	shearzone		all	1	left	
			18	ZZ	1	8	2	left	2 small Z folds on-top of each other

Bag	Depth	Structure	cm scale	Fold type	Thick-ness	Color	No. of Folds	Fold axis ori-ent.	Comment
3278		folding	107	Z	9	7	3	left	
			104	asymmetric fold	1	9	1	left	layers below without effect
			73	Z	5	9	3	left	
			68	Z	1	8	4	left	
			60	Z	30	all	min 4	left	many Z folds
			44	Z	3	7	2	left	
			37 to 35	shearzone		all	2	left	
			18	Z	3	10	4	left	
			10 to 7	shearzone		all	1	left	
3280		folding	96	Z	5	8	1		many Z Folds
			78	Z		all	2		many Z Folds
			70	Z	40	all	1		many Z Folds
			36	Z	5	9	1		many Z Folds
3290		folding							2-3 Z folds per layer
3300	1.815,000								
3310		folding							2-3 Z folds per layer
3316		folding	76	waves	5	7	2	left	
			58	Z	2	6	1	left	

Bag	Depth	Structure	cm scale	Fold type	Thick-ness	Color	No. of Folds	Fold axis ori-ent.	Comment
			49	ripped	4	9			??? What happened here
			47	Z	6	6			
			40	chaos	10	all	1		
3320		folding							2-3 Z folds per layer
3330		folding							2-3 Z folds per layer
3340		folding							
3356		folding	104	Z	3	9	2	left	
			100 to 97	Z		all	3	left	
			94	thickening	30	6	1	left	one Z fold that thickens
			86	Z	2	9	1	left	
			80	Z	1	8	2	left	
			68	Z	8	8	1	left	check 3D
			39	Z	1	8	1	left	
			9	Z	1	7	3	left	

Bag	Depth	Structure	cm scale	Fold type	Thick-ness	Color	No. of Folds	Fold axis ori-ent.	Comment
3360		folding							Z-folding dominant
3370		folding						left	Z-folding and tilting dominant
3380		folding							Z-folds in thin layers
3390		folding							flat Z-folds
3396		folding	100	thickening	5	7			
			92	Z	1	8	2	left	
			88	Z	2	8	2	left	
			77	Z	5	7	1	left	long Z fold, causes thickening
			62	Z	1	9	1	left	
			45	tilting	20 to 13	5		left	
			18	sheared				left	hard to see what happend
			10	Z	5	9	3	left	3 Z waves cause thickening
3400		folding							flat Z-folds
3410		folding							flat Z-folds and tilting

Bag	Depth	Structure	cm scale	Fold type	Thick-ness	Color	No. of Folds	Fold axis ori-ent.	Comment
3420		folding							Z-folds and thick-ness variations
3430		folding							Z-folds and thick-ness variations
3440		folding							Z-folds
3456	1.900,800	folding	106	ZZ	7	all	3	left	
			102	Z and brittle	10	8	1	left	
			92	Z and sheared out	12	all		left	
			67	Z	3	0	1	left	more like a step than a Z fold
			64	ZZZ	2	8	4	left	
			30	ZZZ	25	all	3	left	3 Z folds cause thickening
			4	Z		all	2	left	
3460		folding							Z-folds, bigger 2 cm
3470		folding							many Z-folds per layer
3480		folding							flat Z-folds

Bag	Depth	Structure	cm scale	Fold type	Thick-ness	Color	No. of Folds	Fold axis ori-ent.	Comment
3490		folding							folds and waves
3500		folding							many and long Z-folds
3510		folding							Z-folds across many layers
3520		folding							Z-folds and tilting
3530		folding							flat Z-folds
3540		folding							long Z-folds
3550		folding							Z-folds and waves
3560		folding							long Z-folds
3568		folding, many Z	50	layer stops	5	6	1		layer gets thinned and stops
3570		folding							long Z-folds
3580		folding							long Z-folds and strong tilting
3590		folding							long Z-folds
3596		folding, many Z	107	prop. Fault	30	all	2	right	steep angle
			93	Z	3	8	1		long Z fold

Bag	Depth	Structure	cm scale	Fold type	Thick-ness	Color	No. of Folds	Fold axis ori-ent.	Comment
			87	layer stops	5	6			
			85	waves	10	all	2	right	
			74	asymmetric fold	30	all	3	right	
			66	Z	30	all	many	right	many Z folds
			47	Z	3	5	1	right	Z fold so long, looks like layer stops
			26	fold	50	all	1	right	many normal folds ontop of each other
			0 to 40	check c-axis					
3600		folding							many Z-folds, long but also across many layers
3610		folding							many Z-folds, long but also across many layers

Bag	Depth	Structure	cm scale	Fold type	Thick-ness	Color	No. of Folds	Fold axis ori-ent.	Comment
3620		folding							long Z-folds and strong tilting
3630		folding							long Z-folds
3636		everything wavey	88	layer stops	4	7		right	
			35	Z	5	7	2	right	layer underneth, sig thickening
3638	2.000,900	slight deforma-tion	68	Z	5	7	1	right	very long Z fold?
3650		folding (long Z layers, looks sheared)	103	Z	2	8			thinning of layers at the sides
			89	thinning	2	8			
3700	2.035,000	folding	8	Z and sheared					long Z and waves
3750	2.062,500	folding	84	Z and sheared					strong tilting, many Z

Bag	Depth	Structure	cm scale	Fold type	Thick-ness	Color	No. of Folds	Fold axis ori-ent.	Comment
			52	ZZ	4	5	2		
			33	shearzone	30	all	1	left	
			9	shearzone and Z	min 20	all		left	
3800	2.090,000	folding	99	shearzone and Z	40	all	1	left	increasing prop. Faults (compared to cores above)
			90	Z	5	8	2	left	
			50	shearzone				left	shows all folding and deformation
3850	2.117,500	folding							Z folds and prop.faults, noth-ing significantly important
3876	2.131,800	folding	100	ZZZ				left	
			40	Z	20		1	left	only visible in very bright picture
			20	shearzone	40	all		left	check c-axis
			5	shearzone	40	all		left	check c-axis

Bag	Depth	Structure	cm scale	Fold type	Thick-ness	Color	No. of Folds	Fold axis ori-ent.	Comment
3878		folding (through-out core)	100	Z	20	all	3	left	can be measured for comp.contr.
			90	Z	30	all	1	left	
			75	Z	20	all	2	left	
			37	asymmetric fold	10	3	1	left	
			22	double asym-metric fold	5	7	3	left	very deformed
3880		folding (through-out core)	101	Z	40	all	many	left	
			94	asymmetric fold	15	9	1	left	
			77	waves	10	8	2	left	
			70	shearzone	50	all	1	left	
			60	shearzone	50	all	1	left	
			50	shearzone	50	all	1	left	
			36	shearzone	50	all	1	left	
			15	double Z	20	all	2	left	
			11	double Z	5	7	2	left	

Bag	Depth	Structure	cm scale	Fold type	Thick-ness	Color	No. of Folds	Fold axis ori-ent.	Comment
3882		folding (hardy to see)	55	Z	2	9	1	left	many more folds, but hard to de-scribe
			29	Z	2	8	1	left	many more folds, but hard to de-scribe
			23	Z	10	all	1	left	many more folds, but hard to de-scribe
3884		folding	110	Z	3	10	4	left	4 folds in one layer; many Z folds more or less ontop of each other
			99	thrust fold	10	7	2	left	thrust fold?
			96	shearzone	20	all	1	left	prop. Fault, but more folding inbe-tween
			85	???		all		left	
			72	Z and Wave	3	all	2	left	first Z then wav-ing of layers
			70	detachment fold	8	8	1	left	detachment fold or prop.fault

Bag	Depth	Structure	cm scale	Fold type	Thick-ness	Color	No. of Folds	Fold axis ori-ent.	Comment
			50	Z	1	9	5	left	
			27	Z	1	9	2	left	
			20	shearzone	60	all	2	left	
			14 to 4	Z		all	many	left	many strongly sheared Z folds
3886		shearing							
3888	2.138,400	shearing	100	small waves	10	7	0		
			97	ZZZZZ	2	8	5		5 Z folds ontop of eachother
			67	Z	2	8	3		3 Z folds behind eachother
3890		shearing							waves, Z folds cut through by prop. Faults. Many small folds but layers often end
			90	waves	15	6	many	left	more or less undisturbed
			86	sheared					4 cm later stronly sheared layers
			77	shearzone	40	all	1	left	
			63	Z	16	all	1	left	
			37	Z	10	8	4	left	

Bag	Depth	Structure	cm scale	Fold type	Thick-ness	Color	No. of Folds	Fold axis ori-ent.	Comment
			34	wave and Z	3	9		left	nice example
			20 to 0	Z-fold and shear-zone	40	all	many	left	prop and Z all the way down
3892		folding and shearing	110	wave and Z	2	8	5	left	
			87	ZZ	4	5	2	left	
			76 to 70	wave and Z		all	many	left	many waves and Z folds. Nice to see
			53	Z	4	8	4	left	
			46	Z	3	5	5	left	Z or maybe prop. Faults
3894		folding	104	Z	10	2	1	left	big Z fold
			92	Z	8	7	1	left	
			87 to 80	shearzone		all	3	left	
			80 to 72	shearzone and Z-fold		all	min. 5	left	
			60 to 52	shearzone		all	1	left	just 1 prop. Fault, the rest is well layered

Bag	Depth	Structure	cm scale	Fold type	Thick-ness	Color	No. of Folds	Fold axis ori-ent.	Comment
			56	sheared	4	10	1	left	
			33	shearzone and Z-fold	10	all	4	left	
			26	waves	20	all	5	left	
			22	ZZ	4	10	min 3	left	
			15	shearzone	50	all	2		
			9	Z	5	8	2		
3896		folding	95	Z		7	1	right	
			90	Z		6	1	right	
			86	shearzone	20	all	1	right	
			84	waves	3	8	5	right	
			80 to 74	shearzone		all	2	right	fat prop. Fault
			76	brittle	6	8	1		brittle?
			69	detachment fold	10	all	1		brittle?
			67 to 60	shearzone		all	5		many prop. Faults
			58	shearzone	10	all	2		prop. Fault or de-tachment fold.
			40	shearzone		10		right	
			32	ZZZ	2	7	4	right	

Bag	Depth	Structure	cm scale	Fold type	Thick-ness	Color	No. of Folds	Fold axis ori-ent.	Comment
			27 to 24	ZZZZZ	3	7	min 5		strongly sheared, many Z folds on-top of each other
			22	thrust fold	8	7	1	right	
			19	Z	2	8	2		
			9	waves	40	all	3		
			2	ZZ		6	2		
3898		folding and shearing	110	waves and Z					
			93	Z	5	7	1		big Z fold
			66 to 63	ZZZ		all	many		many Z folds, stronly sheared
			50	overturned fold	3	4	1		
			43 , 5	Z or auf-schiebung	7	8	1		
			28 to 20	shearzone		all	2		
3900		folding	107	Z	10	5	1		flat, nearly prop. Fault

Bag	Depth	Structure	cm scale	Fold type	Thick-ness	Color	No. of Folds	Fold axis ori-ent.	Comment
			106 to 30	Z-fold and shear-zone		all			many Z folds and layers that end
			30	Z	10	8	2		
			13	ZZZZ	5	8	5		
3902			110 to 85	Z-fold and shear-zone		all	many		many Z folds and shearing, hard to specify
			84	ZZZZ					layer ends
			75	ZZZZ	3	9	5		
			50	prop. Fault and Z					super crazy
			37	waves and Z	15	all	many		
			7	Z	4	8	middle		
3904		folding and shearing	110 to 90	sheared					
			90	Z					Z fold with some more shearing
			73	ZZZZ	15	all	many		

Bag	Depth	Structure	cm scale	Fold type	Thick-ness	Color	No. of Folds	Fold axis ori-ent.	Comment
			69	ZZ		all	many		
			53	Z-fold and shear-zone		all	3		
			46	shearzone	30	all			
			42	Z	5	7	1		
			23	Z	10	7	1		
			14	ZZZZ		all	many		
			2	ZZ	4	3	4		
3906	2.148,300	folding	72	Z	15		3	left	
			60	shearzone	30	all	2	left	
			51	Z	10	3	1		check c-axis
3908		folding	110 to 44	shearzone and Z-fold					
			44	ZZZ	8	all	3		
			30 to 20	ZZZZ		all	many		
			15	sheared		all	many		
3910		layering	75	Z	20	9	1		big Z fold, rest layered
			9	sheared	20	all			

Bag	Depth	Structure	cm scale	Fold type	Thick-ness	Color	No. of Folds	Fold axis ori-ent.	Comment
3912	2.151,600	folding	108	Z-fold and thrust		all	1		
			100	Z-fold and shear-zone	5	8	3	left	
			96	Z	5	3	1		
			93	shearzone	10	9	1	left	
			90	thrust fold		all	1		
			80 to 66	sheared					
			60	Z	10	0	1		big Z fold
			58 to 48	sheared					
			43	thrust fold					thrust fold or de-tachment fold
			6	detachment fold					
3920		no visi-ble lay-ering							crystals or folds? Strongly tiltet to the right

Bag	Depth	Structure	cm scale	Fold type	Thick-ness	Color	No. of Folds	Fold axis ori-ent.	Comment
3930	2.161,500	folding	75	asymmetric fold	2	9	2	right	only single layers visible and folded
			48	Z	30	all			strong Z, hard to see
			5	Z	1	9	2		
3940		layering							
3950		no visi-ble lay-ering							
3960	2.178,000	sheared							strong Z folds and shearing and prop. Faults; tilted to the right
3970		sheared							Z and prop. Faults tilted to the right
3980		folded							nice prop. Or de-tachment folds
3990		folded and sheared							hard to see, folded or sheared
4000		sheared							hard to see, sheared

Bag	Depth	Structure	cm scale	Fold type	Thick-ness	Color	No. of Folds	Fold axis ori-ent.	Comment
4004		sheared							sheared but hard to see
4006	2.203,300	sheared							sheared but hard to see
4008		folding							many Z folds but looks like straight layering
4010		folding							many Z folds but looks like straight layering
4020		layered							"layered" flat, lit-tle wavy
4030		layered and crystals							layering in the background and something like crystaly in the foreground
4040		layered and crystals							layering in the background and something like crystaly in the foreground

Bag	Depth	Structure	cm scale	Fold type	Thick-ness	Color	No. of Folds	Fold axis ori-ent.	Comment
4050		sheared and crysals							shearing in the background and something like crystaly in the foreground
4060		sheared and crysals							no layering visible, all sheared
4070		sheared and crysals							no layering visible, all sheared
4080		sheared and crysals							no layering visible, all sheared
4090		sheared							no layering visible, all sheared
4092	2.250,600	big crys-tals							
4100	2.255,000	sheared and crystals							no layering visible, all sheared
4110		sheared							no layering visible, all sheared

Bag	Depth	Structure	cm scale	Fold type	Thick-ness	Color	No. of Folds	Fold axis ori-ent.	Comment
4120		waves, layered, sheared							many Z folds in more or less pral-lel layers
4130		sheared							no layering visi-ble, all sheared
4140		waves, layered, sheared							many Z folds in more or less pral-lel layers
4150		sheared							no layering visi-ble, all sheared
4160		sheared and crystals							no layering visi-ble, all sheared
4170		sheared							no layering visi-ble, all sheared
4180		sheared and crystals							no layering visi-ble, all sheared
4190		sheared and crystals							no layering visi-ble, all sheared
4200		sheared and crystals							no layering visi-ble, all sheared

Bag	Depth	Structure	cm scale	Fold type	Thick-ness	Color	No. of Folds	Fold axis ori-ent.	Comment
4210	2.315,500	sheared							no layering visible, all sheared
4250		crystals							
4300		crystals							
4350		big crys-tals							
4400		no layer-ing visi-ble							
4450		thick layering							?
4500		thick layering							
4546	2.500,300	no visi-ble lay-ering							
4600	2.530,000	big crys-tals							

Table 8.1: A list of bag numbers and depths, the structure and types of folds, cm scale, layer thickness and color, number of folds, the orientation of the shearzone and a comment.